Check for updates

Psychophysiology

WILEY | SPR Society for Psychophysiological Research

ORIGINAL ARTICLE

Multimodal Spatiotemporal Dynamics of Frontomedial Theta and BOLD Signal Reveal Functional Roles in Updating and Suppressing Aversive Memory During Fear Extinction

Arslan Gabdulkhakov[1,2] | Matthias F. J. Sperl[3,4,5] | Christian J. Merz[6] | Laura-Isabelle Klatt[7] | Christoph Fraenz[1] | Erhan Genç[1]

[1]Neuroimaging and Interindividual Differences Unit, Department of Psychology and Neurosciences, Leibniz Research Centre for Working Environment and Human Factors at TU Dortmund (IfADo), Dortmund, Germany | [2]Department of Psychology, Ruhr University Bochum, Bochum, Germany | [3]Department of Clinical Psychology and Psychotherapy, University of Siegen, Siegen, Germany | [4]Department of Clinical Psychology and Psychotherapy, University of Marburg, Marburg, Germany | [5]Department of Clinical Psychology and Psychotherapy, University of Giessen, Giessen, Germany | [6]Department of Cognitive Psychology, Institute of Cognitive Neuroscience, Faculty of Psychology, Ruhr University Bochum, Bochum, Germany | [7]Information Processing Unit, Department of Ergonomics, Leibniz Research Centre for Working Environment and Human Factors at TU Dortmund (IfADo), Dortmund, Germany

Correspondence: Erhan Genç (genc@ifado.de)

Received: 12 July 2025 | **Revised:** 3 February 2026 | **Accepted:** 28 February 2026

Keywords: fear extinction | multimodal neuroimaging | Pavlovian fear conditioning | simultaneous EEG-fMRI | theta | vmPFC

ABSTRACT

Fear and extinction learning are fundamental processes shaping the regulation and expression of fear in both healthy individuals and patients with anxiety-related disorders. Pavlovian fear conditioning serves as a powerful model for these mechanisms; however, the precise spatiotemporal neural dynamics underlying fear and extinction learning in humans still remain unclear. Theta oscillations have been implicated in these learning processes, yet their precise relationship with blood-oxygen-level-dependent (BOLD) signals of corresponding brain networks remains poorly understood. This study employed simultaneous electroencephalography and functional magnetic resonance imaging (EEG-fMRI) in fifty healthy humans to investigate the role of frontomedial theta oscillations (4–8 Hz) in fear learning. Participants underwent a one-day differential fear conditioning paradigm with concurrent EEG and fMRI recordings. We assumed that individual theta power variations would correspond to distinct activation patterns in the fear and safety networks during fear acquisition and extinction training. To test this hypothesis, we extracted frontomedial theta power across three trial segments (0 to 2 s, 2 to 4 s, 4 to 5.5 s after the onset of conditioned stimuli, CS) and integrated these measures into whole-brain fMRI analyses. Results revealed a significant increase in differential (CS+ vs. CS–) theta power toward the end of the CS presentation during fear acquisition training, aligning with prior findings of theta ramping-up before unconditioned stimulus onset. EEG-driven fMRI analyses during fear acquisition showed distinct theta–BOLD co-activations in cuneal and precuneal cortices and motor areas at 2 to 4 s and 4 to 5.5 s trial segments. Notably, during extinction training, the theta activity of the mid-trial segment (2 to 4 s post-stimulus) was co-activated with the BOLD signal in vmPFC, suggesting a role of theta during extinction in safety memory formation. Our findings support the hypothesis that theta oscillations may contribute to the temporal encoding of threat expectation during fear learning, but also to memory updating through fear response suppression during extinction learning. Interestingly, theta modulation was linked to distinct brain regions in different temporal segments. Critically, our results integrate previous findings from different neuroimaging modalities and extend our understanding of the spatiotemporal neural dynamics underlying fear and extinction learning.

© 2026 Society for Psychophysiological Research.

1 | Introduction

The prevalence of anxiety-, trauma-, and stressor-related disorders in modern society underscores the importance of understanding the neural mechanisms underlying fear learning and its regulation (Somers et al. 2006; VanElzakker et al. 2014). The fear conditioning paradigm serves as a well-established model for studying these processes, providing key insights into how fear responses are acquired and extinguished (Lissek et al. 2005; Milad and Quirk 2012; Sehlmeyer et al. 2009; Wake et al. 2024). Recent reviews emphasize that fear conditioning not only serves as a laboratory model for fundamental fear processes but also provides crucial insights into maladaptive fear characteristics underpinning clinical anxiety, including fear generalization and avoidance behaviors that interact with extinction processes, thereby enhancing the translational relevance of this paradigm (Beckers et al. 2023; Hermann and Sperl 2023). In this paradigm, a stimulus (e.g., a tone, shape, or image) is contingently paired with an aversive unconditioned stimulus (US) to become a conditioned stimulus (CS+), in a manner that makes it a reliable predictor of the US, which then leads to a conditioned response (CR). In differential fear conditioning paradigms, another stimulus, the CS−, is never paired with the US and thereby comes to signal its absence (Lonsdorf et al. 2017; Rescorla 1967, 1988; see also Öhman and Dimberg 1978). To induce extinction learning, the same CS+ is repeatedly presented without the US. Over time, this diminishes the CR to the CS+ by creating a new inhibitory memory trace, competing with the initially acquired CS+/US association (Bouton 2002) and/or suppressing the initial CS+/US association. Competing theoretical accounts (for reviews, see Dunsmoor et al. 2015 and Laing et al. 2025) suggest that extinction may reflect the unlearning or modification of the original CS+/US association (Rescorla and Wagner 1972), the formation of a new inhibitory association that suppresses fear expression while leaving the original memory intact (Bouton et al. 2021; Pearce and Hall 1980), or an interaction between both processes. Considering these perspectives helps situate neural findings (such as increases in theta oscillatory activity throughout the course of CS presentation; Starita et al. 2023) in the broader context of whether extinction reflects suppression of the fear response, the formation of a safety memory, or both. Meta-analytic and contemporary learning-theory work further indicate that individuals with anxiety and stress-related disorders show altered fear and safety learning across acquisition, extinction, and recall, with these differences shaped by temperamental vulnerabilities, early learning histories, and contextual influences (Kausche et al. 2025; Zinbarg et al. 2022). This growing recognition of individual differences in learning processes and their neural signatures makes it vital to incorporate subject-specific markers reflecting learning, such as the electroencephalography (EEG) oscillatory activity, in the analysis of neuroimaging data. This would enable a more precise and temporally informed understanding of the brain circuits underlying threat acquisition and extinction, which is crucial for the development of more targeted and effective anxiety treatments. Contemporary neuroimaging research has identified key brain circuits involved in fear acquisition and extinction and their functional role in these processes (Battaglia et al. 2020; Knight et al. 2004; LaBar et al. 1998). These structures include but are not limited to the amygdala, hippocampus, insular cortex, dorsal-anterior cingulate cortex (dACC), and ventromedial prefrontal cortex (vmPFC), constituting the so-called "fear and extinction network" (Fullana et al. 2016; Sehlmeyer et al. 2009). Yet critical questions remain regarding their precise temporal and spatial dynamics, as well as the relationship between findings from different imaging modalities.

For decades, behavioral and electrophysiological studies in animal models dominated the field of fear conditioning, disentangling the functional role of specific anatomical regions related to the conditioning and extinction of fear (Ressler 2020). Rodent prelimbic prefrontal cortex (PL; homologous to the human ACC) and infralimbic prefrontal cortex (IL; homologous to the human mPFC) were shown to be involved in fear expression and suppression, relaying sensory information to the amygdala through so-called "cortical" and "subcortical" pathways (Blair et al. 2001; Burgos-Robles et al. 2009; Milad and Quirk 2002; Pitkanen 2000; VanElzakker et al. 2014). Particularly, theta frequency oscillations were reported to support the communication between the basolateral amygdala and mPFC (Karalis et al. 2016; Likhtik et al. 2014). One of the earliest electrophysiological studies on fear conditioning reported that the hippocampal CA1 region and the lateral amygdala display synchronized theta oscillations during conditioned fear, suggesting that coherent theta activity in amygdalo-hippocampal circuits may promote the synaptic plasticity mechanisms underlying the consolidation and retention of fear memory (Seidenbecher et al. 2003). More recent work has identified the nucleus reuniens (RE) of the thalamus as a critical hub for coordinating mPFC-hippocampus theta synchrony during extinction retrieval: inactivation of RE disrupts both mPFC-hippocampus coherence and extinction memory, whereas theta-paced stimulation of RE restores context-appropriate fear suppression (Totty et al. 2023).

Functional neuroimaging in humans has implicated the amygdala, hippocampus, insula, and prefrontal regions (including the dACC and vmPFC) in the acquisition and extinction of conditioned fear (Büchel and Dolan 2000; Fullana et al. 2016; Kim and Jung 2006; LaBar et al. 1998; Milad and Quirk 2012; Phelps et al. 2004; Sehlmeyer et al. 2009). During fear acquisition, increased functional magnetic resonance imaging (fMRI) blood-oxygen-level-dependent (BOLD) activity is typically observed in the amygdala and dACC, reflecting the encoding and expression of threat-related information. In contrast, extinction learning and recall are associated with enhanced activation of the vmPFC and hippocampus, which are thought to support context-dependent safety learning and inhibition of the previously learned CR (Fullana et al. 2016, 2018; Kalisch et al. 2006; Milad et al. 2007). However, despite numerous individual findings from animal electrophysiology and human neuroimaging studies that helped identify regions constituting the "fear and safety networks", these findings, when taken together, indicate that it is difficult to integrate all known results into a single cohesive interpretation of the involvement of these structures, due to the high heterogeneity of findings across studies. Andres et al. (2024) discuss this issue, particularly in relation to the meta-analysis by Fullana et al. (2018), which did not find consistent vmPFC activation during fear extinction across 31 studies involving 1074 participants. Similarly, meta-analyses have struggled to consistently confirm robust amygdala activation during fear acquisition and extinction (Fullana et al. 2016, 2018). Among

14698986, 2026, 3, Downloaded from https://onlinelibrary.wiley.com/doi/10.1111/psyp.70281 by Erhan Genc - Inst f Arbeitsphysiologie Dortmund , Wiley Online Library on [23/03/2026]. See the Terms and Conditions (https://onlinelibrary.wiley.com/terms-and-conditions) on Wiley Online Library for rules of use; OA articles are governed by the applicable Creative Commons License

other experiment-specific factors, Andres et al. (2024) attribute it to the transient nature of extinction learning activity that might happen only during the first few trials, and temporal dynamics can occur even within a single trial (Miskovic and Keil 2012; Sperl et al. 2021). Thus, although fMRI offers excellent spatial resolution for identifying these distributed circuits, its limited temporal resolution constrains the investigation of rapid neural dynamics involved in fear updating and regulation. Additionally, not much is known about the temporal specificity of respective brain structures during learning. It remains unclear if CS presentations evoke a synchronized BOLD response across all structures or if the functional activation of individual structures changes dynamically throughout each trial.

Complementary to the spatial insights offered by fMRI, EEG studies in humans have provided valuable information about the fast temporal dynamics of fear processing. Event-related potentials (ERPs) such as the late positive potential (LPP) and contingent negative variation (CNV) have been linked to conditioned fear responses and their modulation during extinction (Flor et al. 1996; Miskovic and Keil 2012; Sperl et al. 2021). Electroencephalographic activity can be decomposed into several frequency bands: delta (1–4 Hz), theta (4–8 Hz), alpha (8–13 Hz), beta (13–30 Hz), and gamma (> 30 Hz)—each linked to distinct neural functions. In the context of learning, delta and theta rhythms have been associated with motivational and learning-related processes, alpha oscillations with attentional gating and cortical inhibition, beta activity with sensorimotor integration and expectancy, and gamma oscillations with local network synchronization (Başar et al. 2001; Herrmann et al. 2016; Klimesch 2012). Among these, theta-band activity has received particular attention in emotional learning contexts due to its established role in coordinating information flow between limbic and prefrontal regions during memory encoding and adaptive control (Gilmartin et al. 2014). More recently, oscillatory analyses have provided converging evidence for the role of frontomedial theta as a flexible threat/extinction marker in extinction learning and recall (Bierwirth et al. 2021, 2023; Chien et al. 2017; Mueller et al. 2014; Sperl et al. 2019). An intracranial EEG study in humans reported that theta oscillations in the prefrontal cortex covaried with the progression of learning, thus reflecting the learned association strength (Chen et al. 2021). Additionally, theta frequency oscillations were in synchrony between the amygdala and mPFC, with an increased theta power after successful learning, and the latency of these theta oscillations shifted to earlier time points as learning progressed. However, Clarke et al. (2018) reported opposing results, where the frontomedial theta power decreased as the association strength increased in an associative learning task, suggesting that theta could be linked to establishing the association and, as such, updating the memory.

While the works above focused on the dynamics and progression of learning *across* trials, a scalp EEG study by Starita et al. (2023) analyzed the temporal dynamics of theta power *within* trials. Specifically, they offered a novel approach in discretizing the theta power into three 2-s-long trial segments: 0 to 2 s, 2 to 4 s, and 4 to 6 s relative to CS onset within the trial. Their findings, source-localized to the midcingulate cortex and vmPFC, showed distinct dynamics of the midcingulate theta power across these trial segments in acquisition and reversal phases, with a prominent increase in the differential CS+/CS− effect toward the end of the trial, which could be attributed to threat expectation. An earlier study by DeLaRosa et al. (2014) also reported the dynamics of the distinct topographical distribution of theta and beta power at different time points throughout the trial. Taken together, these findings implicitly hint at the dynamic interplay of various cortical and subcortical structures throughout the learning phase. While EEG source reconstruction provides a practical balance between temporal and spatial resolution, the spatial resolution of EEG source reconstruction is still inferior to that of fMRI (for a broader review of the capabilities of EEG source imaging, see Michel et al. 2004). Hence, a direct link between the transient and temporally specific dynamics of EEG theta power and BOLD signal remains elusive. To date, only a few studies have employed simultaneous EEG-fMRI as part of the fear conditioning paradigm (Sperl et al. 2019; Yin et al. 2020). For example, Sperl et al. (2019) linked oscillatory EEG activity to BOLD responses during extinction recall and reported that frontomedial theta power was significantly reduced for extinguished compared to non-extinguished stimuli, and that this reduction was positively correlated with decreased amygdala BOLD activation. However, the theta–BOLD relationship during fear acquisition and extinction training remains unknown.

Although EEG and fMRI studies have independently advanced our understanding of the temporal and spatial aspects of fear learning, integrated multimodal findings remain scarce, limiting a unified interpretation of underlying neural mechanisms. Simultaneous EEG-fMRI enables a direct validation of modality-specific effects and offers a framework to link temporally defined oscillatory events to spatially distributed brain networks. This integration is especially crucial in learning paradigms, where rapid neural dynamics interact with large-scale circuit activity to shape behavior. The understanding of precise temporal and spatial dynamics of oscillatory activity and brain regions could help establish more robust treatment protocols and inform future brain stimulation studies. Specifically, it is unclear how the fast, oscillatory dynamics captured by EEG relate to the engagement of spatially distinct brain networks as a threat association is processed within a single trial. A CS presentation lasting several seconds is not a monolithic neural event (Miskovic and Keil 2012; Quirk and Mueller 2008), which is reflected in the change of CS+ and CS− difference in theta power throughout the course of CS presentation (Sperl et al. 2019; Starita et al. 2023). Rather, it likely comprises a sequence of distinct cognitive processes, including initial stimulus perception, retrieval of the learned association, threat appraisal, and anticipation of the US (Radua et al. 2025; Wen et al. 2024).

Recent large-scale neuroimaging work provides compelling evidence for such temporal and anatomical specificity. For instance, Wen et al. (2022) demonstrated that transient amygdala BOLD responses during threat conditioning are temporally specific, peaking within the first few trials and habituating rapidly. This finding underscores the principle that averaging neural signals across trials can obscure transient but critical computational processes.

14698986, 2026, 3, Downloaded from https://onlinelibrary.wiley.com/doi/10.1111/psyp.70281 by Erhan Genc - Inst f Arbeitsphysiologie Dortmund , Wiley Online Library on [23/03/2026]. See the Terms and Conditions (https://onlinelibrary.wiley.com/terms-and-conditions) on Wiley Online Library for rules of use; OA articles are governed by the applicable Creative Commons License

Extending this logic from the scale of *across trials* to *within one trial*, it is plausible that different neural circuits are recruited at distinct moments following the onset of a CS. Furthermore, the idea of a single, static "threat circuit" needs to be updated in favor of a more dynamic and distributed model. A comprehensive study by Wen et al. (2024) showed that threat processing engages a wide array of sensory, cognitive, and motor systems beyond the classic "fear network". Crucially, many of these neural nodes dynamically shift their representations of threat (CS+) versus safety (CS−) across different phases of learning, acting as "flexible" coders. If such dynamic engagement of distinct networks occurs over blocks of trials, it strongly suggests that a similar temporal segregation of function could occur on the much finer timescale within a single trial as different cognitive operations are deployed in sequence. This idea has been explored by Starita et al. (2023), showing that the EEG signal, source-localized to the midcingulate cortex, exhibits a distinct increase in theta power across the three discrete temporal segments during the CS presentation. In our study, we extend the above logic and use the subject-specific theta power from the three 2-s-long segments throughout the CS presentation from the scalp EEG as a parametric modulation (PM) regressor in simultaneously recorded whole-brain fMRI. This integrated approach allows us to explore, without prior anatomical constraints, which brain regions (potentially extending beyond the classical "fear and extinction network") are co-activated with EEG-theta at different moments within a trial. As a result, we aim to validate the work of Starita with the EEG signal during acquisition training and extend it to the simultaneously recorded whole-brain fMRI. With the simultaneous recording of EEG and fMRI during extinction learning, we aim to explore whether a similar pattern of within-trial theta dynamics as observed during acquisition emerges, and to determine whether the frontomedial theta effect during extinction is more closely linked to fear or safety network areas.

2 | Materials and Methods

2.1 | Participants

A sample of $N = 50$ (24 women, 26 men) right-handed participants aged between 18 and 26 years ($M = 22.38$ years, SD = 2.35 years) was recruited. The target sample size was informed by the range of sample sizes typically employed in the fear conditioning literature, while accounting for anticipated exclusions due to artifacts from simultaneous EEG-fMRI acquisition. The exclusion criteria at the recruitment stage were a history of mental health conditions, substance or psychoactive medication use, and standard exclusion criteria for fMRI examinations at a 3 Tesla scanner. All participants had normal or corrected-to-normal vision and were able to understand the provided written and oral instructions. All participants were naive to the purpose of the study and had no prior experience with the fear conditioning paradigm used for the experiment. The study was approved by the local ethics committee of the Faculty of Psychology at Ruhr University Bochum (application number 327). All participants provided written informed consent before participation and were treated in accordance with the Declaration of Helsinki. Following the recommendations of Lakens (2022), we conducted a sensitivity analysis using MorePower 6.0 (Campbell and Thompson 2012) to determine the smallest effect size detectable given our final sample and the specific repeated-measures design employed (2 CS types × 3 trial segments). With $N = 35$ (acquisition), assuming 80% power and an $\alpha = 0.05$, the study was sensitive to effect sizes of partial $\eta^2 = 0.13$ or larger. With $N = 39$ for extinction training, the minimum detectable effect size for 80% power was partial $\eta^2 = 0.12$ or larger. In both phases, the sensitivity was sufficient to reliably detect effect sizes comparable to those reported in Starita et al. (2023) with $N = 19$.

2.2 | Experiment

The experiment was conducted at a 3-Tesla Philips Achieva scanner (Philips Healthcare, Best, The Netherlands) equipped with a 32-channel head coil at the Bergmannsheil Hospital in Bochum, Germany. The participants underwent fear acquisition and extinction training on the same day, separated by an 8-min rest period inside the scanner. The stimuli and procedures for these paradigms were adapted from Milad et al. (2007). The stimuli were presented using an MR-compatible display positioned at the back of the MRI bore (BOLDscreen 24 LCD; Cambridge Research Systems, Cambridge, UK). Participants were instructed to pay close attention to the images presented during fear acquisition and extinction training. They were also told that electrical stimulation may or may not be present during the experiment. Fear acquisition training consisted of 32 trials (16 CS+ and 16 CS−), with the CS+ paired with the aversive US in 10 of its 16 trials (62.5% reinforcement rate), followed by extinction training with 8 CS+ (without the US) and 8 CS− trials (see Figure 1). The number of acquisition and extinction trials was selected to be consistent with common experimental designs in human fear conditioning, as documented across numerous studies reviewed by Fullana et al. (2018), ensuring the comparability and applicability of our findings. A single trial commenced with a context presentation for 1 s (AB design, lamp on an office desk during fear acquisition training, lamp on a bookshelf during extinction training). This was followed by a 6 s CS presentation, namely the lamp lighting up in one of two colors: blue or yellow. The US was delivered via a constant voltage stimulator (STM200; BIOPAC Systems, Goleta, CA, USA) and two electrodes attached to the fingertips of the index and middle fingers of the right hand. The stimulation started at 5.9 s after CS onset and co-terminated with the CS+ presentation. The stimulation lasted for 100 ms, consisting of 1 ms pulses at 50 Hz. The US intensity was calibrated individually before the start of the experiment to be rated by participants as "very unpleasant but not painful", starting from 30 Volts (V) and increasing in steps of 5 V ($M = 83.33$ V; SD = 21.65 V). The trials were presented in a pseudo-randomized order, without repeating the same type of trial more than twice in a row. Prior to scanning, all participants were informed that they would be presented with images and may or may not be presented with electrical stimulation during the experiment. After completion of fear acquisition and extinction training, participants filled out a contingency and stimulation rating questionnaire. First, they were asked: 'How many electrical stimulations do you think you received in total during the experiment?' and reported a number. Second, for each CS (blue lamp, yellow lamp), they answered the questions: 'On what percentage of blue lamp presentations was an electrical stimulation delivered?' and 'On what percentage of yellow lamp presentations was an electrical stimulation delivered?' (0–100% in steps of 10%).

14698986, 2026, 3, Downloaded from https://onlinelibrary.wiley.com/doi/10.1111/psyp.70281 by Erhan Genc - Inst f Arbeitsphysiologie Dortmund , Wiley Online Library on [23/03/2026]. See the Terms and Conditions (https://onlinelibrary.wiley.com/terms-and-conditions) on Wiley Online Library for rules of use; OA articles are governed by the applicable Creative Commons License

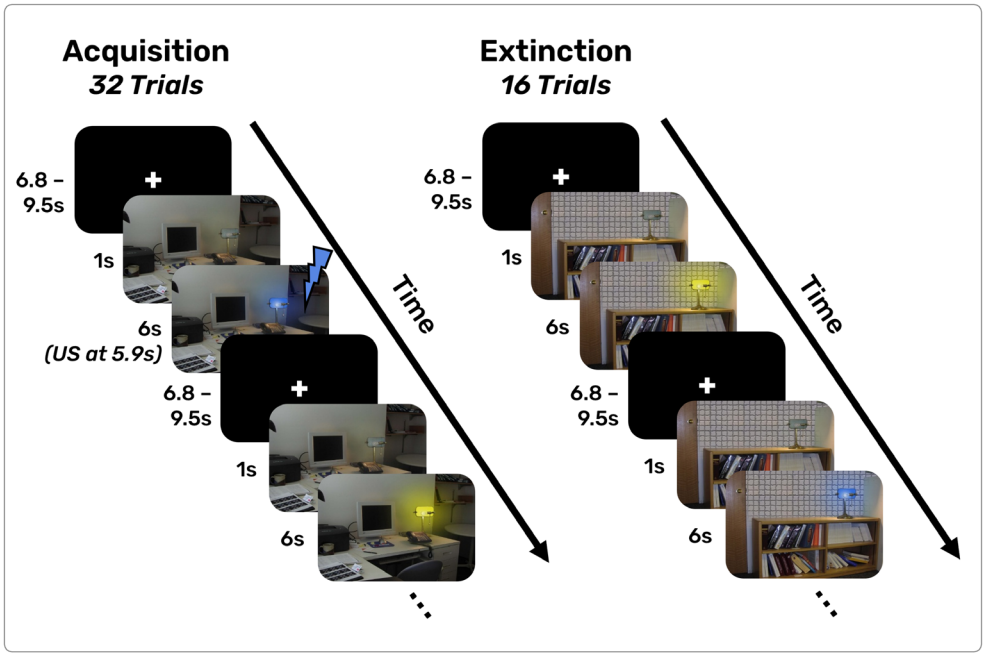

FIGURE 1 | Experimental outline of fear acquisition (left panel) and extinction (right panel) training. *US* = unconditioned stimulus. Both fear acquisition and extinction training started with a fixation cross, which was also presented between trials during an intertrial interval (ITI). The ITI duration jittered from 6.8 to 9.5 s. Following the ITI, a context—an office table with a lamp in acquisition, and a bookshelf with a lamp in extinction—was presented for 1 s. Then, the lamp color, which lit up with either blue or yellow color for a duration of 6 s, signaled either a CS+ or CS− trial. The US, delivered as an electrical stimulation to the right hand, was administered for a duration of 100 ms, starting at 5.9 s after CS+ onset and terminating with CS+ offset. We used a pseudo-randomized partial reinforcement rate of 62.5%; thus, 10 out of 16 CS+ trials during acquisition training were paired with the US.

2.3 | Skin Conductance Response Recording and Analysis

Subjects' skin conductance responses (SCRs) were measured using an additional channel (GSR-MR sensor; Brain Products, Munich, Germany) of the EEG amplifier (see below). Two Ag/AgCl electrodes, each containing an isotonic 0.05 M NaCl electrolyte solution, were placed on the hypothenar area located below the little finger of the left hand. Data were recorded using the Brain Vision Recorder software (version 1.23.0003; Brain Products, Munich, Germany) with a sampling rate of 5000 Hz.

The SCR data were preprocessed to remove scanner artifacts (the specific preprocessing steps are described in Section 2.4) and exported into MATLAB (version R2022b; MathWorks, Natick, MA, USA) for further preprocessing in the EDA-App (Otto et al. 2023). The SCRs were defined as the maximum amplitude values, determined via a foot-to-peak analysis, starting within a 1 to 6.5 s window relative to CS onset. We chose a relatively longer window, which extends the commonly used 1 to 4 s interval recommended by Boucsein et al. (2012), to capture anticipatory responses throughout the entire CS presentation interval in our long-CS paradigm and to align the SCR scoring with the later trial segments analyzed in EEG and fMRI (4 to 6 s post-CS onset; see Sections 2.4 and 2.5). Consistent with the systematic comparison by Kuhn et al. (2022), who show that longer, full-trial windows can perform similarly to narrower windows and that no universally optimal latency window exists, our choice was thus guided by the specific temporal structure of our task. A minimal response criterion of 0.01 μS was applied, consistent with common guidelines (Boucsein et al. 2012). Responses below this threshold were scored as zero, indicating non-responses, and were included in subsequent analyses to preserve the full range of individual variability. No additional standardization or scaling procedures (e.g., range correction or z-scoring) were applied to the SCR amplitudes. This decision reflects our focus on interindividual differences in electrodermal activity, as standardization can reduce meaningful variability and complicate interpretation in studies assessing individual differences. The CR was defined as the difference between the across-trial average SCR values for CS+ and CS− for each participant. After preprocessing, the SCR data were exported for subsequent statistical analyses. Due to excessive residual scanner artifacts or a low signal-to-noise ratio (SNR), a number of participants had to be excluded to maintain data quality, resulting in a final sample of $N = 35$ for acquisition and $N = 32$ for extinction.

2.4 | EEG Recording and Analysis

The EEG data were recorded using an MR-compatible 64-channel BrainCapMR system (Brain Products, Munich, Germany) with an additional electrocardiogram (ECG) channel. The electrode array consisted of the following channels, which were positioned according to the 10–20 system: AF3, AF4, AF7, AF8, C1, C2, C3, C4, C5, C6, CP1, CP2, CP3, CP4, CP5, CP6, CPz, Cz, F1, F2, F3, F4, F5, F6, F7, F8, FC1, FC2, FC3, FC4, FC5, FC6, Fp1, Fp2, Fpz, FT10, FT7, FT8, FT9, Fz, O1, O2, Oz,

14698986, 2026, 3, Downloaded from https://onlinelibrary.wiley.com/doi/10.1111/psyp.70281 by Erhan Genc - Inst f Arbeitsphysiologie Dortmund , Wiley Online Library on [23/03/2026]. See the Terms and Conditions (https://onlinelibrary.wiley.com/terms-and-conditions) on Wiley Online Library for rules of use; OA articles are governed by the applicable Creative Commons License

P1, P2, P3, P4, P5, P6, P7, P8, PO3, PO4, PO7, PO8, POz, Pz, T7, T8, TP10, TP7, TP8, and TP9. The AFz and FCz electrodes were used as ground and reference electrodes, respectively. Data were recorded at a 5000 Hz sampling frequency. A SyncBox (Brain Products, Munich, Germany) was used to synchronize the scanner clock with the EEG system, to ensure a precise gradient marker estimation for correct gradient artifact removal.

The recorded EEG and SCR data were cleaned from gradient (GA) and cardioballistic artifacts (BCG) using Brain Vision Analyzer (version 2.2; Brain Products, Munich, Germany), following procedures described by Allen et al. (1998, 2000). The GA was removed using the average artifact subtraction method (AAS). We visually compared the two approaches, one using the recorded scanner volume markers and the other using the gradient marker detection method, based on the recommendations from Brain Products Support Team, as well as the guidelines for scanner artifact removal in Brain Vision Analyzer (Brain Products 2022). The parameters for the gradient marker detection method were set to 6000 μV/ms, and channel F6 was selected for detection. For certain EEG recordings where detection was not feasible with channel F6, we used other frontal channels. The value of 6000 was adjusted downwards or upwards for some recordings when necessary for a proper gradient marker estimation. The template artifact for both GA correction approaches was constructed using the default 21 intervals for sliding average calculation. The latter approach, in which we used a detection method, resulted in better GA removal and thus better signal-to-noise ratio (under visual assessment), which we then adopted. Following the GA removal, the ECG channel was used to find the R-peaks semiautomatically with Brain Vision Analyzer to correct for BCG artifacts. We used a detection range of 40–90 pulses per minute and adjusted this range upwards for certain subjects with a higher heart rate. All the marked R-peaks were visually inspected for all subjects and manually adjusted if necessary. Analogous to the procedure used for GA removal, an average pulse curve was subtracted from the EEG. Following the BCG correction, the EEG channels were high-pass filtered at 0.5 Hz with a 50 Hz notch filter to remove line noise. The Infomax Independent Component Analysis (ICA) was fitted to detect and remove eye-related artifacts (blinks and saccades) manually. Bad channels were identified manually, rejected, and interpolated. All channels were then re-referenced to the average reference. Trials were visually inspected for remaining artifacts and rejected if necessary ($M_{\text{Acquisition}} = 1.82$ rejected trials, $\text{SD}_{\text{Acquisition}} = 2.46$ rejected trials; $M_{\text{Extinction}} = 0.88$ rejected trials, $\text{SD}_{\text{Extinction}} = 1.02$ rejected trials). One participant for acquisition training and two participants for extinction training were rejected at this stage due to more than half of either CS+ or CS− trials being noisy. Using the wavelet method (5-cycle width) as implemented in the FieldTrip package (version 20220104; Oostenveld et al. 2011), participants' time-frequency representations (TFR) were computed from −4 to 8 s (in steps of 0.05 s) and from 2 to 30 Hz (in steps of 0.5 Hz). All trials were then dB-normalized with a baseline period from −2.3 to −1.3 s relative to CS onset—an interval within the ITI during which a fixation cross was presented.

The per-subject frontomedial theta values were defined as the average of F1, Fz, and F2 electrodes in the range of 4 to 8 Hz (Mueller et al. 2014; Sperl et al. 2019). They were computed for 3 distinct trial time segments relative to CS onset: 0 to 2 s, 2 to 4 s, and 4 to 5.5 s. The last segment was chosen to be 0.5 s shorter to avoid potentially confounding effects of the US, which was delivered at 5.9 s post-CS onset. The per-subject frontomedial theta averages for 16 CS+ and 16 CS− trials, respectively, were exported for further analysis and modeling with the fMRI General Linear Model (GLM). These approximately 2-s-long windows of theta power also allowed us to link the EEG theta signal to the fMRI BOLD signal. To this end, we incorporated respective theta averages as a parametric modulation regressor in whole-brain fMRI GLM analyses, allowing us to link transient electrophysiological activity with slower-evolving BOLD responses. To ensure high data quality in all modalities, we visually inspected whether participants' data exhibited strong movement artifacts in EEG and/or fMRI, or poor ECG quality. As a result, a total of 15 participants' fear acquisition data and 11 participants' fear extinction data had to be excluded from further analyses.

In addition to the main analysis described above, we conducted an exploratory analysis for trial segments, in which fear acquisition and extinction training were subdivided into first and second halves, operationalized as the first and last 8 CS+ and 8 CS− trials each during fear acquisition training and the first and last 4 CS+ and 4 CS− trials each during extinction training. The detailed results are reported in Figure S1.

2.5 | (f)MRI Recording, Analysis, and EEG-fMRI Integration

For coregistration, T1-weighted high-resolution MP-RAGE anatomical images were acquired with the following parameters: TR = 8.2 ms, TE = 3.7 ms, flip angle = 8°, 220 slices, matrix size = 240 mm x 240 mm, resolution = 1 mm x 1 mm x 1 mm. Scanning time was around 6 min.

During fear acquisition and extinction training, fMRI BOLD responses were obtained using echo planar imaging with the following parameters: TR = 2500 ms, TE = 35 ms, flip angle = 90°, 40 slices, matrix size = 112 mm x 112 mm, resolution = 2 mm x 2 mm x 3 mm. The scanning time was approximately 8 min for fear acquisition training and 4 min for extinction training.

The BOLD data were preprocessed using FEAT from the FSL toolbox (version 6.0.1; Jenkinson et al. 2011; Smith et al. 2004). Preprocessing steps included correcting for head motion (MCFLIRT) and slice timing, with a 6 mm FWHM Gaussian kernel for spatial smoothing and a high-pass filter with a cutoff of 50 s. A 6 mm kernel was chosen as it represents a commonly used compromise between increasing signal-to-noise ratio and maintaining spatial specificity, while also accounting for intersubject anatomical variability in group analyses (Mikl et al. 2008). Each BOLD image was linearly registered to the participant's high-resolution T1-weighted anatomical scan, followed by linear registration to the Montreal Neurological Institute (MNI) standard template with 12 degrees of freedom. A total of four participants with strong movement or suboptimal coverage were removed from consecutive analyses. To ensure comparability across modalities, analyses were restricted to participants with good quality data in both EEG and fMRI, resulting in a final sample of $N = 35$ for acquisition and $N = 39$ for extinction.

14698986, 2026, 3, Downloaded from https://onlinelibrary.wiley.com/doi/10.1111/psyp.70281 by Ethan Genc - Inst f Arbeitsphysiologie Dortmund , Wiley Online Library on [23/03/2026]. See the Terms and Conditions (https://onlinelibrary.wiley.com/terms-and-conditions) on Wiley Online Library for rules of use; OA articles are governed by the applicable Creative Commons License

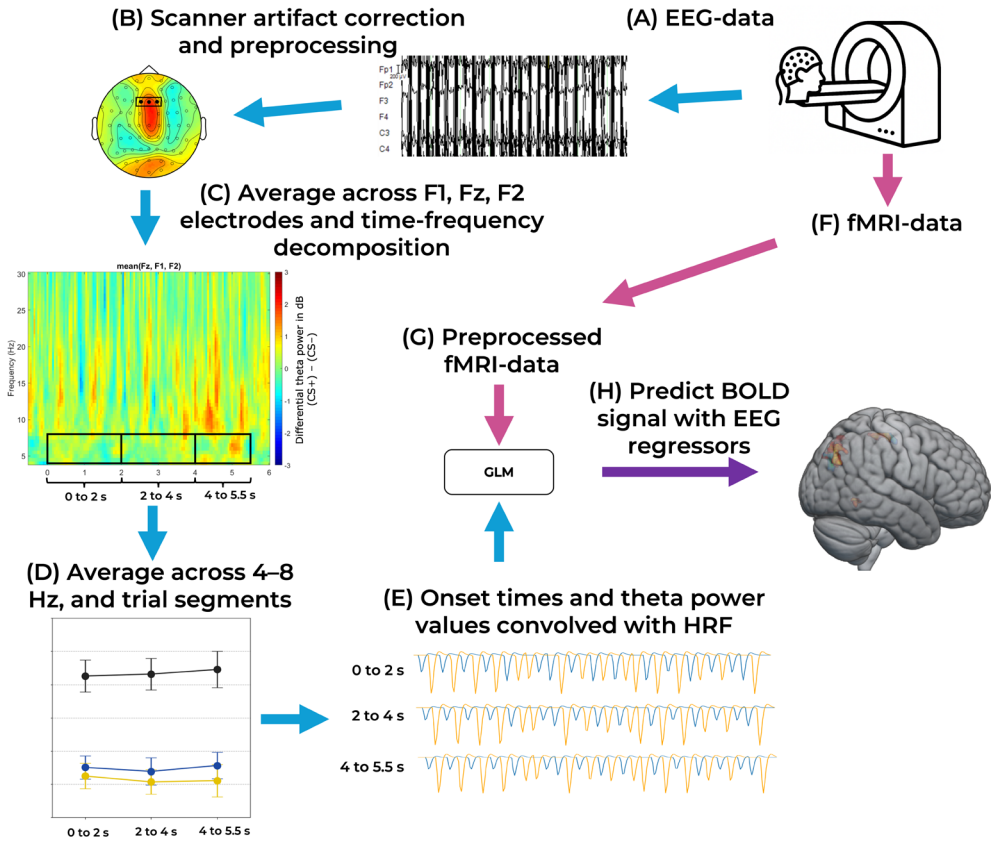

FIGURE 2 | Overview of the EEG-fMRI analysis and integration pipeline, in which the EEG-derived metric (theta power) was entered as a first-level parametric modulation regressor in the fMRI general linear model (GLM); in this article, this is referred to as the "first approach". The figure outlines analysis steps for a single participant, which were repeated for all subjects before the group analysis. *Please note that for visualization purposes, the topographic plot, the differential time-frequency plot, and the average of trial-segment plot show the grand-average of all subjects during extinction training; however, they were modeled with the fMRI GLM on the first level with each participant's individual theta values in the actual analysis.* (A) marks the start of the EEG-analysis part; (B) correction of gradient-, cardioballistic-, and ocular artifacts and filtering; (C) time-frequency decomposition was performed on data averaged across frontomedial electrodes (F1, Fz, F2); (D) theta power (4–8 Hz) was averaged across three trial segments post-CS onset (0 to 2 s, 2 to 4 s, 4 to 5.5 s) for CS+ and CS− conditions separately; (E) the individual participants' average theta power values were convolved with the hemodynamic response function (HRF), separately for CS+ and CS− trials, to generate parametric regressors; (F) simultaneously acquired fMRI data were preprocessed; (G) EEG-theta derived regressors were included in general linear models (GLMs) as predictors; (H) resulting first-level statistical maps per participant were then analyzed on the group level separately for each trial-segment.

For the whole-brain EEG-informed fMRI modeling, we implemented two distinct approaches: (1) we used per-subject theta averages (collapsed across trials within condition and time segment) as parametric modulation (PM) regressors at the first level; and (2) we used the same per-subject average theta values as covariates at the second level, following the method outlined by Sperl et al. (2019). As a reference, we also conducted a conventional fMRI analysis without incorporating EEG data, reported in Figure S2. The preprocessing parameters in FEAT were identical across all approaches. In each model, we included the following task-related regressors in the GLM: the onsets of CS+ and CS− trials, the onset of the context, the US delivery time point following a reinforced CS+ trial (acquisition only), and an analogous time point following the unreinforced CS+ as well as the CS− trials. The CS+ and CS− regressors were contrasted at the first-level GLM to examine condition-related BOLD differences in both EEG-fMRI approaches and the fMRI-only approach. The specifics and the key differences of the two EEG-driven-fMRI analyses are described below.

In the first approach, we averaged the frontomedial theta values within CS+ and CS− trials for each subject and used the average CS+ and average CS− theta values (i.e., one value per condition per subject per trial segment) as PM regressors on the first-level GLM (see Figure 2). Specifically, we ran three distinct analyses for fear acquisition and extinction training for the following three post-CS time windows: 0 to 2 s, 2 to 4 s, and 4 to 5.5 s. The event onsets in FEAT were shifted to match the trial timing from which the EEG data were taken (Figure 2). The event duration was set to 0.1 s, consistent with the event-related design. The regressors for CS+ and for CS− were convolved with the canonical hemodynamic response function (HRF) and modulated by each participant's individual theta value. All second-level analyses were performed using FLAME (FMRIB's Local Analysis of Mixed Effects) to estimate random effects. The second-level contrasts included the individual CS+ and CS− trial onset events, as well as their contrasts: CS+ > CS−, CS− > CS+.

The second approach followed the EEG-fMRI integration methodology outlined by Sperl et al. (2019), using subject-level,

14698986, 2026, 3, Downloaded from https://onlinelibrary.wiley.com/doi/10.1111/psyp.70281 by Erhan Genc - Inst f Arbeitsphysiologie Dortmund , Wiley Online Library on [23/03/2026]. See the Terms and Conditions (https://onlinelibrary.wiley.com/terms-and-conditions) on Wiley Online Library for rules of use; OA articles are governed by the applicable Creative Commons License

trial-segment-averaged theta value differences as a second-level covariate for the CS+ > CS− and CS− > CS+ first-level contrasts. Similar to the first approach, we ran three first-level models for fear acquisition and extinction training (0 to 2 s, 2 to 4 s, and 4 to 5.5 s trial segments). In contrast to the first approach, EEG theta values were not included as parametric modulators at the first level. Instead, each subject's mean normalized CS+/CS− theta difference was entered as a covariate at the second level. This analysis did not yield any significant effects and is therefore not reported further.

After the first-level analysis, the second-level models (group level) for both approaches were analyzed with FLAME 1, applying cluster thresholding with a z-statistic threshold of 3.1 (Eklund et al. 2016) and $p < 0.05$. The significant clusters were mapped to brain areas using the Jülich Histological Atlas and the Harvard-Oxford Cortical and Subcortical Atlases, as implemented in FSL. The significant statistical maps are visualized using the MRIcroGL tool (version 2022-07-20; Rorden 2025).

2.6 | Statistical Analyses

Statistical analyses were conducted in IBM SPSS Statistics 29 (IBM, Armonk, NY, USA). To test the significance of the self-report scores, a t-test was used for the reported percentage of electrical stimulations received after CS+ and after CS− trials. For SCRs, repeated-measures analysis of variance (ANOVA) was conducted with the within-subjects factors CS type (CS+ vs. CS−) and time (first half of trials vs. second half of trials) and their interaction. The alpha level was set to 0.05 for all analyses. For EEG theta power, a repeated-measures ANOVA was computed with the within-subjects factors CS type (CS+ vs. CS−), trial segment (0 to 2 s, 2 to 4 s, 4 to 5.5 s), and their interaction.

The assumptions of the ANOVAs were assessed. Sphericity was evaluated with Mauchly's test and, where violated, Greenhouse–Geisser corrected results are reported. The distribution of residuals was inspected to verify the normality assumption (Lumley et al. 2002). Effects with $p < 0.05$ were considered statistically significant and were followed up with Bonferroni-corrected post hoc tests. Exploratory comparisons that were not supported by a significant omnibus effect are reported in the Supporting Information and clearly identified as exploratory. Following the procedures and guidelines described by Lakens (2013) and Steiger (2004), all ANOVA results are reported with partial η^2 effect sizes and their 90% confidence intervals (CI). For significant post hoc comparisons, descriptive statistics (means, standard deviations) and 95% CI for the mean differences (Bonferroni-corrected) are reported.

3 | Results

3.1 | Contingency Self-Report Scores

The analysis of self-report scores obtained after fear acquisition training revealed successful fear learning. Participants reported receiving an average of 10.12 (SD = 3.41) electrical stimulations, aligning with the 10 stimulations over 16 CS+ trials. Likewise, the average reported percentage of electrical stimulation (US) received after the CS+ ($M = 54.5\%$, SD = 18.19) was significantly higher than after the CS− ($M = 7.98\%$, SD = 15.53, $t(48) = 11.32$, $p < 0.001$, Cohen's $d = 1.61$). The mean reported values closely approximated the actual reinforcement rates of 62.5% for CS+ and 0% for CS−. For extinction training, all participants correctly reported that they received 0 electrical stimulations.

3.2 | Skin Conductance Responses (SCRs)

3.2.1 | Acquisition Training

A repeated-measures ANOVA was conducted to assess the effects of CS type (CS+ vs. CS−), time (first half of trials vs. second half of trials), and the CS type × time interaction on SCRs during fear acquisition training (Figure 3). The analysis revealed a significant main effect of CS type, $F(1, 34) = 15.31$, $p < 0.001$, partial $\eta^2 = 0.311$, 90% CI [0.10, 0.47], and a significant main effect of time, $F(1, 34) = 13.33$, $p = 0.001$, partial $\eta^2 = 0.282$, 90% CI [0.09, 0.45]. The CS type × time interaction was not significant, $F(1, 34) = 0.244$, $p = 0.624$, partial $\eta^2 = 0.007$, 90% CI [0.00, 0.11].

Bonferroni-corrected post hoc test showed that SCRs were significantly higher for CS+ ($M = 0.40$, SD = 0.42) than CS− ($M = 0.23$, SD = 0.27) during the first half of acquisition training ($p < 0.001$, 95% CI [0.09, 0.27]) as well as during the second half of acquisition training (CS+: $M = 0.28$, SD = 0.38; CS−: $M = 0.12$, SD = 0.23; $p = 0.006$, 95% CI [0.05, 0.26]).

3.2.2 | Extinction Training

An analogous repeated-measures ANOVA was conducted for extinction training. The main effect of CS type was not significant, $F(1, 31) = 1.93$, $p = 0.175$, partial $\eta^2 = 0.058$, 90% CI [0.00, 0.22]. A significant main effect of time was observed, $F(1, 31) = 6.99$, $p = 0.013$, partial $\eta^2 = 0.184$, 90% CI [0.02, 0.36], reflecting a general decrease in SCRs across extinction trials. The CS type × time interaction was not significant, $F(1, 31) = 0.01$, $p = 0.921$, partial $\eta^2 = 0.000$, 90% CI [0.00, 0.17]. Bonferroni-corrected post hoc tests confirmed that CS+ and CS− did not differ significantly during either the first half ($p = 0.363$) or the second half ($p = 0.264$) of extinction training, reflecting successful extinction of CR to CS (Figure 3).

3.3 | EEG: Frontomedial Theta Power

3.3.1 | Acquisition Training

A 2 (CS type: CS+ vs. CS−) × 3 (trial segment: 0 to 2 s, 2 to 4 s, 4 to 5.5 s) repeated-measures ANOVA on frontomedial theta power (defined as an average across F1, Fz, F2 electrodes, spanning 4–8 Hz; see Figure 4 for topographical distribution of the theta power and the location of F1, Fz, and F2 electrodes) revealed a significant main effect of CS type, $F(1, 34) = 7.95$, $p = 0.008$, partial $\eta^2 = 0.190$, 90% CI [0.03, 0.36], and a significant CS type × trial segment interaction, $F(2, 33) = 3.47$, $p = 0.043$, partial $\eta^2 = 0.174$, 90% CI [0.01, 0.33]. The main effect of trial segment was not significant, $F(2, 33) = 0.315$, $p = 0.732$, partial $\eta^2 = 0.019$, 90% CI [0.00, 0.10].

14698986, 2026, 3, Downloaded from https://onlinelibrary.wiley.com/doi/10.1111/psyp.70281 by Erhan Genc - Inst f Arbeitsphysiologie Dortmund , Wiley Online Library on [23/03/2026]. See the Terms and Conditions (https://onlinelibrary.wiley.com/terms-and-conditions) on Wiley Online Library for rules of use; OA articles are governed by the applicable Creative Commons License

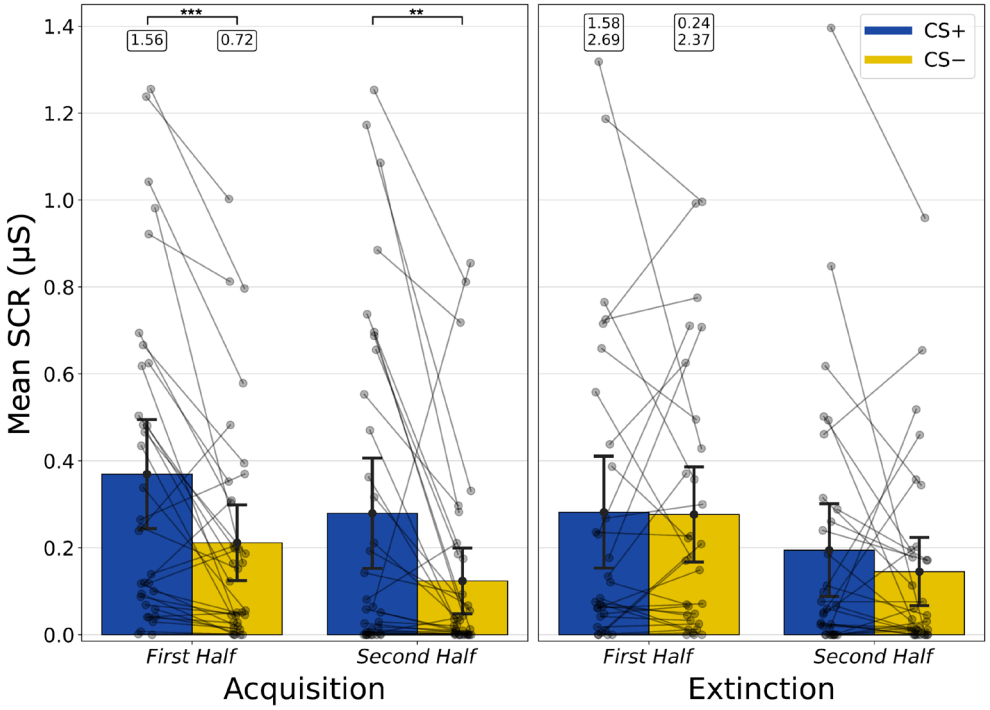

FIGURE 3 | Skin conductance responses (SCRs) for CS+ and CS− during the first and second halves of fear acquisition and extinction training. Mean SCRs (in microSiemens, µS) were calculated separately for acquisition (averaged across the first and last 8 CS+ and 8 CS− trials each) and extinction (averaged across the first and last 4 CS+ and 4 CS− trials each). Bars represent group means, error bars indicate 95% confidence intervals, and gray circles represent individual participants connected across CS+ and CS− conditions. Outlier participants with SCR values exceeding the 1.4 µS threshold in either CS+ or CS− are shown in paired boxes above the bar plots (i.e., both values of the corresponding participant are displayed in the same row). Asterisks denote significant differences (***$p < 0.001$, **$p < 0.01$).

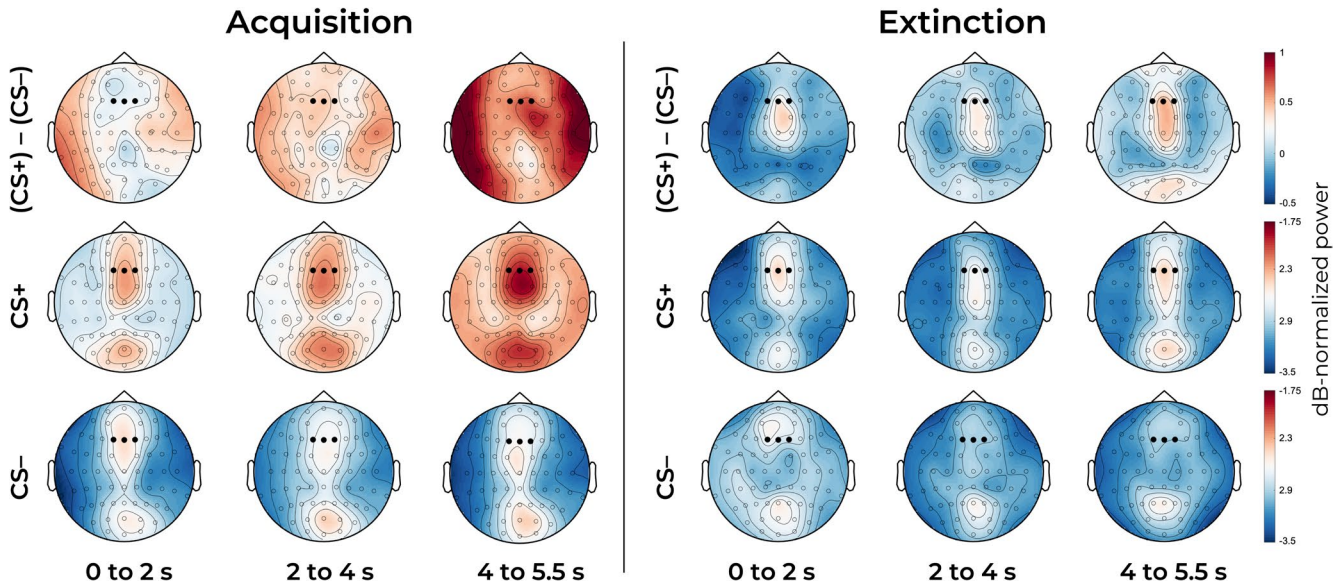

FIGURE 4 | Topographic distribution of EEG theta power (4–8 Hz) during fear acquisition and extinction training. Scalp maps are shown separately for CS+, CS−, and their difference (CS+ − CS−) across three trial time windows (0 to 2 s, 2 to 4 s, and 4 to 5.5 s post-CS onset). The three black dots indicate the F1, Fz, and F2 electrodes, which define the frontomedial region used for averaging and subsequent analyses. Color intensity represents theta power in decibels (dB), with consistent color scales across time windows within each condition to allow comparability (ranges from −0.5 to 1 for the differential (CS+) − (CS−) topographies, and from −3.5 to −1.75 for CS+ and CS− in both acquisition and extinction). Note that although frontal and posterior midline activity is clearly visible, fixed color bar limits (used to ensure comparability) may cause some of these effects to appear visually attenuated.

14698986, 2026, 3, Downloaded from https://onlinelibrary.wiley.com/doi/10.1111/psyp.70281 by Erhan Genc - Inst f Arbeitsphysiologie Dortmund , Wiley Online Library on [23/03/2026]. See the Terms and Conditions (https://onlinelibrary.wiley.com/terms-and-conditions) on Wiley Online Library for rules of use; OA articles are governed by the applicable Creative Commons License

Bonferroni-corrected post hoc tests showed that theta power was significantly higher for CS+ than CS− at 2 to 4 s (CS+: $M = -2.20$, SD = 0.84; CS−: $M = -2.64$, SD = 0.91; $p = 0.012$, 95% CI [0.11, 0.77]) and at 4 to 5.5 s trial segments (CS+: $M = -1.99$, SD = 1.00; CS−: $M = -2.71$, SD = 0.81; $p = 0.004$, 95% CI [0.24, 1.21]) but not at the 0 to 2 s trial segment (CS+: $M = -2.29$, SD = 0.77; CS−: $M = -2.52$, SD = 0.77; $p = 0.158$, 95% CI [−0.09, 0.55]).

To further test whether the CS+ vs. CS− difference increased across trial segments (the expected "ramping-up effect"), Bonferroni-corrected post hoc tests of difference scores (CS+ minus CS−) between consecutive time windows were conducted. The increase was significant from 0 to 2 s ($M = 0.23$, SD = 0.94) to the interval 4 to 5.5 s ($M = 0.72$, SD = 1.40; $p = 0.035$, 95% CI [−0.96, −0.03]). This pattern is consistent with a progressive ramping-up of theta power differentiation between CS+ and CS− during acquisition, in line with previous work (Starita et al. 2023). Differences between other trial segments (i.e., 0 to 2 s compared with 2 to 4 s and 2 to 4 s compared with 4 to 5.5 s) did not reveal significant effects (all ps > 0.05).

3.3.2 | Extinction Training

An analogous 2 × 3 repeated-measures ANOVA on theta power during extinction training revealed no significant main effect of CS type, $F(1, 38) = 2.21$, $p = 0.145$, partial $\eta^2 = 0.055$, 90% CI [0.00, 0.20], no significant main effect of trial segment, $F(2, 37) = 1.31$, $p = 0.283$, partial $\eta^2 = 0.066$, 90% CI [0.00, 0.20], and no CS type × trial segment interaction, $F(2, 37) = 0.48$, $p = 0.625$, partial $\eta^2 = 0.025$, 90% CI [0.00, 0.11]. Complementary ramp-up analyses revealed no significant increase in the CS+ vs. CS− difference across any time window during extinction (all ps > 0.05).

Prior studies suggest that participants' behavior as well as neurocognitive correlates change from the first to the second half of fear acquisition and extinction training (e.g., see Åhs et al. 2015; Graner et al. 2020; Sperl et al. 2021). To further investigate whether differential CS+/CS− theta power is more prominent during the first or the second halves of fear acquisition and extinction training, we exploratively split the trials into first and second halves (see Figure S1). Similar to our results reported above, we found the difference between CS+ and CS− to be significant for trial segments at 2 to 4 s and 4 to 5.5 s in the first but not the second half of fear acquisition training. This highlights that the ramping-up effects observed and reported in Figure 5 are mainly driven by the first half of fear acquisition training. In the case of extinction training, we observed the opposite pattern: the difference between the CS+ and CS− showed a trend in the late, but not in the first half of extinction training.

3.4 | Conventional fMRI Analysis Without EEG Parameters

The conventional fMRI analysis revealed a significant activation in the dACC for the CS+ > CS− contrast during acquisition training, with the peak activation voxel at $x = 2$; $y = 22$; $z = 32$, and a z-statistic value at the peak voxel of 4.21 (see Figure S2). No other contrasts were significant in this analysis without EEG parameters, i.e., neither the CS− > CS+ contrasts for acquisition or extinction, nor the CS+ > CS− contrast for extinction. However, a recent publication by Fraenz et al. (2025) with an

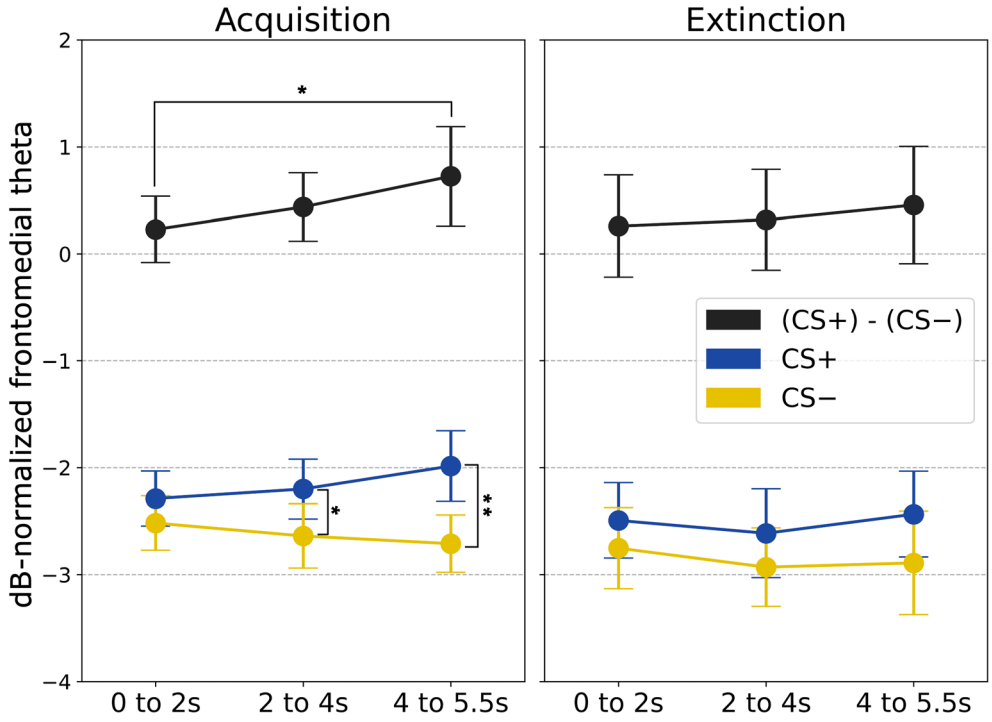

FIGURE 5 | dB-normalized EEG theta dynamics from frontomedial electrodes (F1, Fz, and F2) during fear acquisition and extinction training across three trial segments (0 to 2 s, 2 to 4 s, and 4 to 5.5 s post-CS). The error bars indicate 95% confidence intervals around the mean. The significant CS+ > CS− differences in specific trial segments, and the significant increase in the differential theta effect between trial segments, are marked with asterisks (**$p < 0.01$, *$p < 0.05$).

14698986, 2026, 3, Downloaded from https://onlinelibrary.wiley.com/doi/10.1111/psyp.70281 by Erhan Genc - Inst f Arbeitsphysiologie Dortmund , Wiley Online Library on [23/03/2026]. See the Terms and Conditions (https://onlinelibrary.wiley.com/terms-and-conditions) on Wiley Online Library for rules of use; OA articles are governed by the applicable Creative Commons License

identical paradigm but a larger ($N = 126$) sample, shows major activations across the so-called "fear and safety networks", overlapping with the meta-analysis maps from Fullana et al. (2016).

We performed an additional whole-brain analysis on the effects of the US delivery (i.e., the unconditioned response) after the reinforced CS+ trials, contrasting it with a comparable time point in CS− trials during fear acquisition training, which allowed us to test the effectiveness of the US stimulation. We found robust activations across multiple threat- and pain-related regions that have previously been linked to threat processing, namely in the bilateral insular cortices, dACC, left precentral gyrus, bilateral angular gyri, left primary somatosensory cortex, bilateral opercula, and major cerebellar activations (see Figure S3). Importantly, the activation in the left primary somatosensory cortex during the US delivery period (middle axial slice in Figure S3), shows, as anticipated, a contralateral response to the US, which was delivered to the right hand.

3.5 | Simultaneous EEG-fMRI Results

Overall, the EEG-driven fMRI analysis revealed significant theta–BOLD co-activation spanning the known "fear and safety networks" during fear acquisition (see Figure 6 and Table 1) and extinction training (see Figure 7 and Table 1). During fear acquisition training, for the trial segment at 0 to 2 s post-CS onset, we did not find any significant theta–BOLD co-activation. For the trial segment at 2 to 4 s, the bilateral primary motor and right somatosensory cortices, right inferior parietal lobule PGp and left inferior parietal lobule PGp/7A, left cuneal and precuneal cortices, as well as regions from the left visual cortex (V2–V4), were significantly co-active for the CS+ > CS− contrast (see Figure 6 and Table 1). For the trial segment at 4 to 5.5 s, significant clusters in the right primary motor cortex, the left superior parietal lobule 7A, and left cuneal cortex were co-active with EEG theta for the CS+ > CS− contrast (see Figure 6 and Table 1). For the CS− > CS+ contrasts, we did not find significant co-activation in all trial segments of acquisition training.

During extinction training, we found for the trial segment 2 to 4 s that the left vmPFC exhibited a theta–BOLD co-activation for the contrast CS+ > CS− (see Figure 7 and Table 1). In light of the prominent role of the vmPFC for extinction learning (Milad and Quirk 2012), this might point toward a role of frontomedial theta in the extinction of aversive memories. We did not observe significant theta–BOLD co-activations for either the 0 to 2 s or the 4 to 5.5 s segment for the CS+ > CS− contrast.

We also found a significant theta-BOLD co-activation for the CS− > CS+ contrast in the extinction training at the 0 to 2 s trial segment in the left precentral gyrus and premotor cortex (see Figure 8 and Table 1). The CS− > CS+ contrasts in other trial segments were not significant.

4 | Discussion

In this study, we investigated the temporal dynamics of frontomedial theta, defined as the average over F1, Fz, and F2 electrodes in the 4–8 Hz range, during fear acquisition and extinction training using simultaneous EEG-fMRI. Consistent with Starita et al. (2023), we observed a ramping-up of the theta power difference between CS+ and CS− throughout the fear acquisition trials. Theta–BOLD coupling during fear acquisition shifted from parietal and occipital regions (2 to 4 s post-CS) to motor areas (4 to 5.5 s), reflecting different stages of threat encoding. During extinction training, theta-driven BOLD coupling was confined to the vmPFC in the mid-segment (2 to 4 s), pointing to a temporally specific role for frontomedial theta in updating aversive memory representations. Together, these results confirm our assumptions about the temporal specificity of functional activation in different brain structures during fear conditioning and extinction.

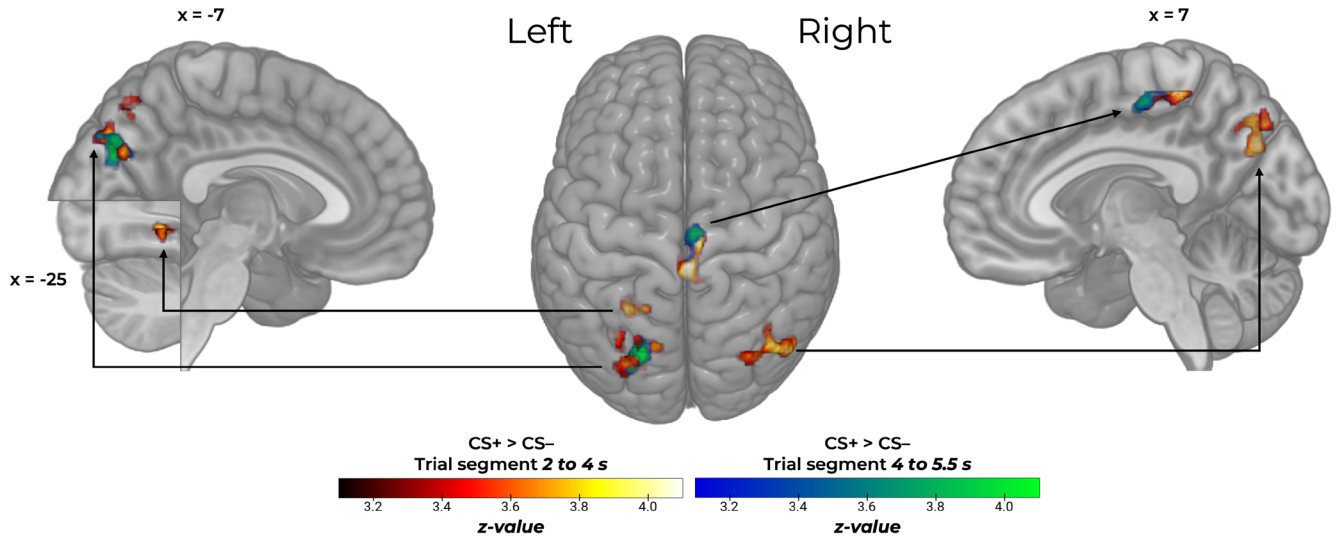

FIGURE 6 | EEG-theta–BOLD co-activation for CS+ > CS− during fear acquisition training, across the 2 to 4 s and 4 to 5.5 s trial segments, plotted on the transparent MNI152 template. Red-to-yellow (left color bar) indicates a significant cluster during the 2 to 4 s trial segment for the CS+ > CS− contrast. Blue-to-green (right color bar) indicates a significant cluster during the 4 to 5.5 s trial segment for the CS+ > CS− contrast. For the 0 to 2 s trial segment, no significant theta–BOLD co-activation occurred. The color bars code the thresholded z-statistic values from 3.1 to 4.1.

14698986, 2026, 3, Downloaded from https://onlinelibrary.wiley.com/doi/10.1111/psyp.70281 by Erhan Genc - Inst f Arbeitsphysiologie Dortmund , Wiley Online Library on [23/03/2026]. See the Terms and Conditions (https://onlinelibrary.wiley.com/terms-and-conditions) on Wiley Online Library for rules of use; OA articles are governed by the applicable Creative Commons License

TABLE 1 | Overview of the MNI coordinates for the peak cluster activation points related to theta–BOLD co-activation.

Phase	Time (s)	Contrast	Area	MNI coordinates			*z*-stat.
				x	*y*	*z*	
Acquisition	0 to 2	CS+ > CS−	Not significant	—	—	—	—
Acquisition	0 to 2	CS− > CS+	Not significant	—	—	—	—
Acquisition	2 to 4	CS+ > CS−	**Bilateral primary motor cortices and right primary somatosensory cortex**	1.9	−35.6	57.9	4.4
			Left V2-V4	−25.5	−54.0	−5.8	4.3
			Right inferior parietal lobule PGp	46.3	−72.2	34.6	4.3
			Left inferior parietal lobule PGp/7A	−22.4	−76.2	34.3	4.2
			Left cuneal cortex/left precuneal cortex	−12.3	−72.0	30.0	4.0
Acquisition	2 to 4	CS− > CS+	Not significant	—	—	—	—
Acquisition	4 to 5.5	CS+ > CS−	**Right primary motor cortex**	4.2	−19.7	53.9	4.2
			Left superior parietal lobule 7A and left cuneal cortex	−21.9	−74.0	32.1	4.7
Acquisition	4 to 5.5	CS− > CS+	Not significant	—	—	—	—
Extinction	0 to 2	CS+ > CS−	Not significant	—	—	—	—
Extinction	0 to 2	CS− > CS+	**Left precentral gyrus and premotor cortex**	−24.0	−10.3	49.9	3.9
Extinction	2 to 4	CS+ > CS−	**Left vmPFC**	−11.5	40.3	−4.2	4.1
Extinction	2 to 4	CS− > CS+	Not significant	—	—	—	—
Extinction	4 to 5.5	CS+ > CS−	Not significant	—	—	—	—
Extinction	4 to 5.5	CS− > CS+	Not significant	—	—	—	—

Note: The areas highlighted in bold are the brain regions according to anatomical atlases (Jülich Histological Atlas and the Harvard-Oxford Cortical and Subcortical Atlases).
Abbreviations: *7A*, area 7 anterior; *PGp*, parietal area G posterior; *vmPFC*, ventromedial prefrontal cortex.

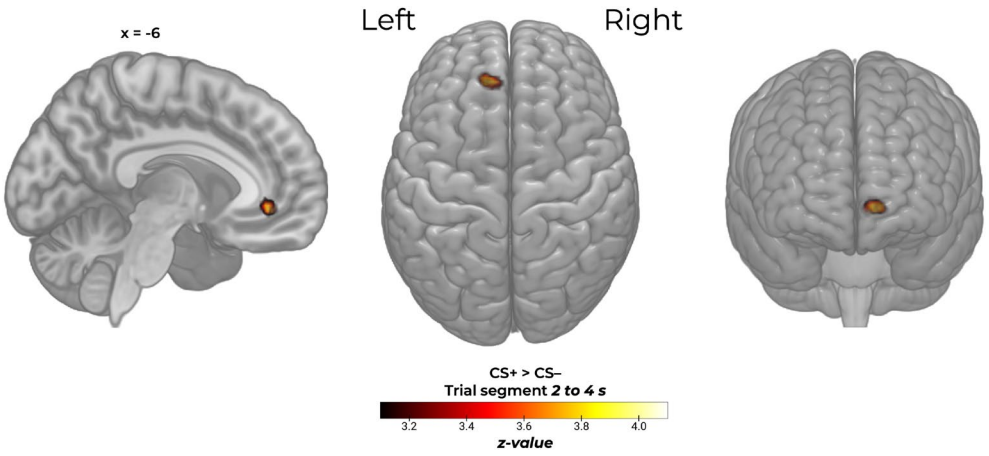

FIGURE 7 | EEG-theta–BOLD co-activation for the CS+ > CS− contrast during extinction training in the 2 to 4 s trial segment, plotted on the transparent MNI152 template. Red-to-yellow indicates a significant cluster during the 2 to 4 s trial segment for CS+ > CS−. This cluster spans the left vmPFC. No significant effects occurred in the other trial segments. The color bar codes the thresholded *z*-statistic values from 3.1 to 4.1.

Self-report ratings and SCRs both confirmed that participants successfully acquired and extinguished conditioned fear. As expected, SCR results showed a robust CS+ > CS− differentiation during the first and second halves of the acquisition training and no significant differential effect in both halves of extinction.

It is important to note that extinction training in our paradigm was conducted in a different visual context than acquisition (AB design). This choice was made to facilitate the translational applicability of our findings to real-life scenarios of exposure therapy, which usually takes place in a different context from the

14698986, 2026, 3, Downloaded from https://onlinelibrary.wiley.com/doi/10.1111/psyp.70281 by Erhan Genc - Inst f Arbeitsphysiologie Dortmund , Wiley Online Library on [23/03/2026]. See the Terms and Conditions (https://onlinelibrary.wiley.com/terms-and-conditions) on Wiley Online Library for rules of use; OA articles are governed by the applicable Creative Commons License

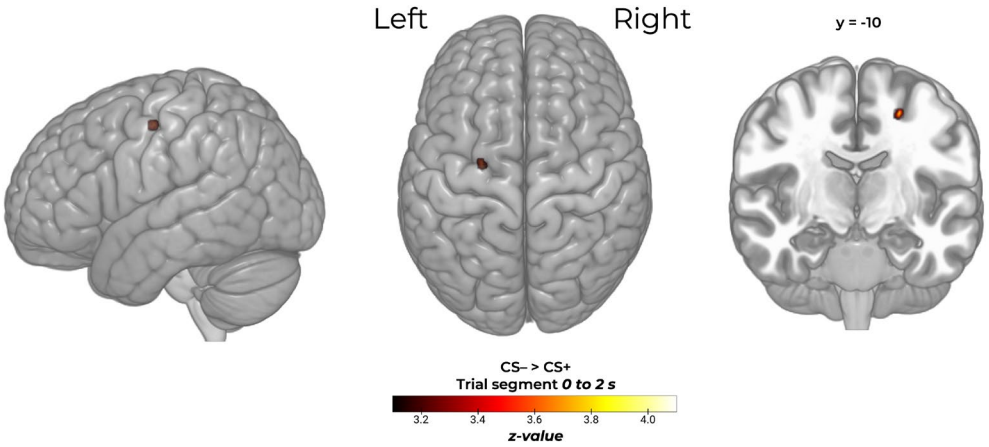

FIGURE 8 | EEG-theta–BOLD co-activation for the CS– > CS+ contrast during extinction training in the 0 to 2 s trial segment, plotted on the transparent MNI152 template. Red-to-yellow indicates a significant cluster during the 0 to 2 s trial segment for CS– > CS+. This cluster is centred at the left precentral gyrus. No significant effects occurred in the other trial segments. The color bar codes the thresholded *z*-statistic values from 3.1 to 4.1.

one in which aversive associations have been acquired (see, for example, Beckers et al. 2023). This transition between phases, marked by both an 8-min rest period and the context change, likely signaled a new and ambiguous situation for participants. We interpret the increase in SCRs to both CS+ and CS− during early extinction as evidence of generalized arousal in response to the context shift and phase transition (see Figure S4). This interpretation is in line with work showing that context shifts can alter SCRs independently of associative learning (e.g., elevated or altered responding following a context change; Sjouwerman et al. 2015). Separately, latent-cause models of conditioning suggest that such contextual changes can encourage learners to assign extinction trials to a new latent state with its own learning history (Gershman et al. 2010). We therefore view our data as consistent with the idea that context changes may both elicit non-associative arousal and alter the inferred state of the task, though the generalized arousal and the latent-cause inference reflect fundamentally different mechanisms. Crucially, however, the temporal progression of SCRs across trials shows that despite this initial, elevated response, SCRs to both the CS+ and CS− diminished by the end of the session (see Figure S4). Importantly, the time course of responding to the CS+ is more fluctuant compared to a steady decrease in responding toward the CS–, confirming successful extinction learning and thus indeed associative processes. Fluctuations might reflect the partial reinforcement rate between CS+ and US during fear acquisition training. Still, results regarding the initial extinction trials also argue for an involvement of non-associative arousal, such as generalized arousal and/or context-induced interference. Finally, we note that extinction training comprised fewer trials than fear acquisition training, following earlier paradigms in human fear conditioning research (e.g., Phelps et al. 2004; Milad et al. 2007). While this choice ensures comparability with prior work, recent methodological guidelines now recommend using longer or dynamically adjusted extinction training phases to better capture the full time course of fear attenuation (e.g., Lonsdorf et al. 2017). This difference in trial numbers should be considered when interpreting the extinction-related findings of the present study.

Frontomedial theta effects (Figure 5) during acquisition training in our sample confirmed the ramping-up effects reported by Starita et al. (2023), robustly demonstrating the role of theta frequency in threat expectation, especially near US delivery (2 to 4 s and 4 to 5.5 s post-CS onset). Exploratory analyses splitting acquisition training into first and second halves (Figure S1) revealed that the differential theta effect toward trial end is primarily driven by the first half of acquisition, while the effect plateaus during the second half, potentially due to habituation to the US (Sperl et al. 2016) if theta tracks threat. Interpreting these findings alongside Clarke et al. (2018), who show that frontomedial theta power drops as association strength increases, we propose that frontomedial theta facilitates CS+/US association formation, predominantly in early acquisition, as a wiring mechanism bridging their temporally disconnected onsets. This interpretation is further supported by animal studies (Karalis et al. 2016; Likhtik et al. 2014; Seidenbecher et al. 2003) and our own exploratory results (Figure S1) show that significant frontomedial theta differentiation in the first half of trials disappears in the second half. Although habituation could account for the absence of a differential CS+/CS− EEG theta effect later in acquisition (Figure S1; Sperl et al. 2016), the sustained differential CS+/CS− effect in SCR data across both halves (Figure 3) counters this explanation. This dissociation between EEG and SCR patterns motivates extending the interpretation to extinction learning, where the differential CS+/CS– effects in SCR emerge only in the initial trials (Figure S4), whereas the differential CS+/CS– theta effects appear only in the later trials (Figure S1). Together, these findings suggest that frontomedial theta activity may not solely reflect threat expectation but also processes related to fear regulation and suppression during extinction learning. These findings, however, should be interpreted cautiously given the limited trial numbers, underscoring the need for future studies using finer temporal scales or single-trial analyses, such as representational similarity analysis (Kriegeskorte et al. 2008), with larger samples.

While we did not find a significant CS+ > CS− effect in the EEG theta averaged across all trials during extinction training

14698986, 2026, 3, Downloaded from https://onlinelibrary.wiley.com/doi/10.1111/psyp.70281 by Erhan Genc - Inst f Arbeitsphysiologie Dortmund , Wiley Online Library on [23/03/2026]. See the Terms and Conditions (https://onlinelibrary.wiley.com/terms-and-conditions) on Wiley Online Library for rules of use; OA articles are governed by the applicable Creative Commons License

(Figure 5), a similar exploratory analysis as for the acquisition, where we analyzed the first and second halves of extinction trials (4 CS+ and 4 CS− trials each), showed a comparable theta ramping-up effect during the second but not the first half of extinction training (see Figure S1), with the 4 to 5.5 s trial segment being significant for CS+ > CS−. Note that we did not observe a significant ANOVA main effect for stimulus type during the late extinction with our sample (only at trend-level: $p = 0.066$), indicating that the robustness of these effects during extinction requires further investigation. Nevertheless, consistent with transient extinction phenomena documented in humans (LaBar et al. 1998; Phelps et al. 2004), our interpretation is that participants need several trials without the US in the new context before recognizing the shift. By the second half of extinction trials (trials 5–8), fear is likely suppressed and/or a new safety memory is being formed—indicated by the return of the theta ramping-up effect, potentially marking an update in CS contingency. Accordingly, we propose that theta facilitates CS+/US associations during early acquisition and may support the formation of new safety memories or the suppression of old aversive associations during later extinction. However, it is important to note that competing theoretical accounts of extinction propose different mechanisms underlying this process. Extinction may involve either the modification of the original CS+/US memory ("unlearning"), the formation of a new inhibitory association that suppresses fear expression, or a dynamic interplay between both mechanisms (Bouton et al. 2021; Gershman et al. 2017; Pearce and Hall 1980; Rescorla and Wagner 1972). The vmPFC activation observed concurrently with theta modulation during extinction aligns with prior work implicating this region in the balance between these mechanisms, mediating the suppression of fear while enabling flexible retrieval of safety associations. The findings of the conventional fMRI-only analysis (Figure S2) showed a rather classical activation in the dACC for the CS+ > CS− contrast during acquisition, which is consistent with earlier studies (see Fullana et al. 2016, 2018, for example). Though no other significant activation has been observed for the classical fMRI analysis in this simultaneously recorded EEG-fMRI sample, a recent publication from our lab with the identical paradigm and a bigger sample with 126 individuals (see figures S7 and S8 of Fraenz et al. 2025) has shown a broader activation in the relevant fear and safety networks.

With our EEG-driven fMRI analysis, we found distinct activation patterns across the brain at different trial segments during fear acquisition training for the CS+ > CS− contrast. Specifically, activation was observed in the left cuneal and precuneal regions, the left and right segments of the inferior parietal lobule, as well as the left visual, bilateral motor, and right somatosensory cortices at 2 to 4 s relative to the CS onset. The theta-modulated BOLD responses at the 4 to 5.5 s trial segment were exhibited in the right primary motor cortex, left cuneal cortex, and the left superior parietal lobule. This partially overlapped with the activation observed at the 2 to 4 s segment; however, other structures active at 2 to 4 s were no longer engaged. The involvement of cuneal and precuneal cortices during the 2 to 4 s trial segment, together with visual cortex structures, might indicate multimodal sensory integration and again confirm the interpretation of Starita et al. (2023) on the role of theta in threat expectation during fear learning. However, in contrast to our findings, this area has primarily been reported in previous studies during extinction training (Fullana et al. 2016; Phelps et al. 2004; Wen et al. 2021). For instance, Wen et al. (2021) interpreted precuneus activation (part of the default mode network) as reflecting the integration of otherwise segregated sensory and cognitive systems to support the complex demands of extinction learning. However, as suggested by Andres et al. (2024), the functional role of brain structures previously believed to be specific to threat or safety processing may need to be re-evaluated. For example, Battaglia et al. (2020) reported that participants with vmPFC lesions failed to produce conditioned physiological responses as a result of acquisition training—suggesting a necessary re-evaluation of the role of vmPFC beyond extinction training. Although our findings do not overlap with the source-localized regions reported by Starita et al. (2023), this discrepancy is not surprising since we explored the co-activation of subject-specific theta values and the BOLD signal across all voxels in the whole brain, in contrast to a theory-driven subset of anatomical brain regions. Likewise, by using EEG theta as a parametric modulation regressor in the fMRI BOLD analysis, we aimed to directly link the two imaging modalities, whereas source localisation techniques, used in the original paper by Starita et al. (2023), serve a different purpose: mapping scalp-level EEG activity to the anatomical locations of its underlying generators. Importantly, the shift from parietal and occipital brain structures at 2 to 4 s to clearer motor activations at 4 to 5.5 s might reflect the initiation of motor responses for fight-or-flight behavior in anticipation of threat (see Mobbs et al. 2007, 2009). Therefore, we note that the effects observed in the late temporal window (4 to 5.5 s post-CS onset) may not be exclusively driven by learning or memory processes but are also likely influenced by expectation and contingency processes. Though our goal was to link theta activity to regions in the whole brain, future studies might benefit from employing a similar approach but with predefined regions of interest (ROI) analyses, as the high resolution of 3 T fMRI could have prevented local activations in other regions from surviving the multiple comparisons correction.

During extinction training, we found a significant theta-modulated BOLD response in the vmPFC solely during the 2 to 4 s trial segment, which highlights a potential temporal specificity of vmPFC activation relative to CS onset. Taken together with our finding that the differential theta power effects emerged during the second half of extinction training, these results may align with the 6–9 Hz effects reported by Totty et al. (2023), which were shown to mediate mPFC-hippocampal connectivity in mice. Additionally, the inconsistency of vmPFC activation during extinction learning in earlier work (Andres et al. 2024; Fullana et al. 2018) may be attributable to the temporal specificity of vmPFC engagement, which might be averaged out if an entire trial period was chosen for analysis. Thus, our data suggest that studies failing to detect vmPFC involvement during extinction likely used analysis windows that did not encompass the critical interval at 2 to 4 s post-CS onset in which theta-modulated vmPFC activation emerged in our sample. Across the physiological modalities, the SCR results showed a reduction in the differential CS+/CS− effect in the second half of extinction, while exploratory EEG results show an increase in differential CS+/CS− induced theta in the second half of extinction, and our EEG-informed fMRI results indicate theta-modulated vmPFC activation. We interpret that these findings suggest an involvement of theta activity during extinction learning by supporting

14698986, 2026, 3, Downloaded from https://onlinelibrary.wiley.com/doi/10.1111/psyp.70281 by Erhan Genc - Inst f Arbeitsphysiologie Dortmund , Wiley Online Library on [23/03/2026]. See the Terms and Conditions (https://onlinelibrary.wiley.com/terms-and-conditions) on Wiley Online Library for rules of use; OA articles are governed by the applicable Creative Commons License

an update of the original memory. Specifically, theta may promote learning of a new association—namely, that the CS+ no longer signals the US—and the suppression of fear responses, as indicated by reduced differential SCRs to the CS.

Interestingly, the theta–BOLD co-activation in the precentral gyrus and premotor cortex at the 0 to 2 s trial segment of extinction training was the only significant effect among all trial segments across both experimental phases for the CS− > CS+ contrast. Given the heightened SCR to CS− trials in the first half of extinction, this effect may reflect an expectancy of CS+/US contingency reversal in a novel context, as described above. Taken together with the robust theta–BOLD co-activation for CS+ > CS− and the timing of these effects, our findings suggest that frontomedial theta is more closely tied to threat-related processing than to safety signaling.

While classical threat-conditioning studies often report activation in the dACC and insula, (e.g., Radua et al. 2025; Wen et al. 2024), we did not observe significant responses in these regions for the CS+ > CS− contrast in the EEG-driven fMRI results. Nor did we detect amygdala activation, consistent with the notion that its engagement in human threat conditioning remains debated (Visser et al. 2021; Wen et al. 2022). Although our analysis employed a whole-brain approach, detecting activity within smaller subcortical structures such as the amygdala would require a dedicated ROI analysis, which would deviate from the exploratory, whole-brain framework adopted here. Future studies could complement this approach with targeted ROI analyses to further examine the contribution of these structures to theta–BOLD coupling. It is therefore important to note that the EEG-driven fMRI approach applied here is not a conventional whole-brain method but rather a special data-fusion technique emphasizing voxels whose BOLD time courses covary with fluctuations of frontomedial theta. Consequently, the analysis selectively highlights cortical regions whose activation is temporally coupled with theta oscillations, rather than providing an exhaustive picture of all fear-related activity in the brain. From this perspective, the absence of typical "fear network" activations during fear learning may indicate that frontomedial theta dynamics at different trial segments reflect processes other than canonical threat expression, possibly a neural correlate of threat expectation or attentive monitoring of aversive contingencies, as previously suggested by Starita et al. (2023). Although our exploratory EEG results warrant caution, they point to a potentially pivotal role of frontomedial theta across fear acquisition and extinction learning—supporting CS+/US association formation during acquisition and updating this association during extinction. Moreover, the prominent vmPFC activation observed in our EEG-informed fMRI analyses during extinction suggests that this same theta rhythm may shift functionally toward regulating fear suppression or promoting the formation of safety memory, consistent with prior accounts of midline-prefrontal involvement in extinction and safety retrieval (Wen et al. 2021; Zhang et al. 2025). These interpretations, however, should be regarded as tentative. Future studies with larger samples and higher fMRI field strength at 7 Tesla, permitting layer-specific and connectivity-informed analyses, will be essential to clarify whether frontomedial theta exerts a top-down influence on cortical and subcortical nodes of the "fear and safety networks", or instead reflects a downstream readout of these processes. This could provide a more mechanistic interpretation of whether the theta–BOLD co-activation in vmPFC during extinction learning supports more the fear suppression, safety memory formation, or both processes simultaneously.

Although this study aimed to combine the temporal precision of EEG with the spatial resolution of fMRI to leverage the strengths of both modalities, each method individually presents challenges for directly linking EEG signals to the BOLD response (for a review, see Abreu et al. 2018). Of particular importance is the low signal-to-noise ratio of the EEG and the necessity of having a large number of repetitions, which are then averaged to enhance the signal quality (Luck 2014). While this method works well in sensory-motor experiments, learning processes, which are characterized by a dynamic change between trials during the course of each learning phase, might be too transient and be averaged out over the course of many repetitions (Sperl et al. 2021), and participants may even habituate to the aversiveness of the stimuli (Sperl et al. 2016). Earlier work in the associative learning experiment by Hanslmayr et al. (2011), who attempted to relate trial-by-trial theta activation to the BOLD signal with parametric modulation, did not yield any significant results. Therefore, to establish a direct relationship between the BOLD signal and EEG spectral components, we averaged across all EEG trials for each participant, trading off *across*-trial temporal resolution in favor of capturing *within*-trial dynamics in the EEG-fMRI integration. Also, our additional approach to adopt the methodology of Sperl et al. (2019)—linking EEG theta activity to the BOLD signal at the second-level group analysis—did not yield any significant results. However, in light of our combined EEG-fMRI results and previous EEG work (e.g., Starita et al. 2023), we see the necessity of studying the EEG-fMRI relationship on a longer time scale, beyond the short periods post-CS onset, as the activation pattern changes dynamically throughout the trial. By adopting the approach from Starita et al. (2023), we artificially split data into three 2-s segments, but the true theta–BOLD relationship may occur on even narrower time segments. This warrants future research to explore indirect fusion methods for the two modalities, applying techniques such as representational similarity analysis (RSA; Kriegeskorte et al. 2008). Specifically, this method could enable the linking of similarity measures from EEG data on time scales both between and within trials—shorter than the 2 s trial segments—while also allowing for a division of trials into first and second halves. On the other hand, an extension of our approach of EEG-fMRI integration as a parametric modulation, but with EEG-theta averaged from temporally shorter segments (with 1 or 0.5 s trial segments, for example), could possibly reveal even finer, temporally specific activation in the BOLD signal, though segments too short (i.e., too few cycles per segment) could lead to inaccurate estimation of the frequency effects (Cohen 2014).

In the present work, we focused specifically on the theta frequency range (4–8 Hz) because of its well-established role in orchestrating communication between frontal and limbic regions during learning and memory processes (Cavanagh and Frank 2014; Karalis et al. 2016). Converging evidence links

14698986, 2026, 3, Downloaded from https://onlinelibrary.wiley.com/doi/10.1111/psyp.70281 by Erhan Genc - Inst f Arbeitsphysiologie Dortmund , Wiley Online Library on [23/03/2026]. See the Terms and Conditions (https://onlinelibrary.wiley.com/terms-and-conditions) on Wiley Online Library for rules of use; OA articles are governed by the applicable Creative Commons License

frontomedial theta to the encoding of aversive predictions (Chen et al. 2021; Sperl et al. 2019), and adaptive control (Cavanagh and Frank 2014; Cohen and Donner 2013), functions that are central to threat and extinction learning. Other frequency bands, such as alpha, beta, or gamma, may also contribute to fear learning by indexing inhibitory or attentional mechanisms (see Herrmann et al. 2016; Klimesch 2012; Mueller et al. 2014; Panitz et al. 2019), yet their coupling with BOLD activity remains largely unknown. This leaves room for future studies to examine broader spectral–BOLD relationships across multiple frequency bands to provide a more comprehensive understanding of how oscillatory networks support fear acquisition and extinction. Such investigations could elucidate whether theta–BOLD interactions represent a unique mechanism of affective learning or form part of a wider spectrum of frequency-specific neural dynamics.

Likewise, future studies combining EEG and fMRI simultaneously during fear acquisition and extinction training at higher MRI field strengths, which provide higher spatial resolution, and with more trials in both acquisition and extinction, may help clarify the directionality of the effects we reported. For example, whether vmPFC activation—building on results from animal models (Milad and Quirk 2012)—enables the extinction of fear memories by suppressing amygdala activation, and how this mechanism might relate to theta oscillations, remains elusive. ROI analyses, as opposed to whole-brain analyses in our study, could help in answering this question. Lastly, future fMRI-only studies with bigger samples might find distinct activation patterns in the brain at different trial segments relative to the CS onset, but also across the trials, to uncover the learning dynamics throughout the experiment. This could potentially untangle the brain structures comprising the so-called "fear and safety networks" and link activation of individual brain structures to specific time points throughout the experiment. Taken together, these findings would support a view of extinction learning as a dynamic process that integrates both suppression of the original fear response and the formation of new safety memories. The temporal specificity of theta–vmPFC coupling (as observed in our data) may thus mark the neural instantiation of this interplay.

In conclusion, this study demonstrates that frontomedial theta power during fear and extinction learning reflects temporally dynamic neural processes that are linked to distinct brain regions. Ramping-up of theta power (for CS+ relative to CS− stimulation) corresponds to somatosensory engagement during threat anticipation in acquisition training, while theta–vmPFC co-activation during extinction learning suggests involvement in updating aversive memory representations. Our findings highlight the value of combining EEG and fMRI to uncover the spatiotemporal mechanisms underlying both fear and extinction learning. Future work may build on this foundation by investigating neuromodulatory or clinical interventions targeting these processes.

Author Contributions

Arslan Gabdulkhakov: methodology, software, investigation, writing – original draft, writing – review and editing, visualization. **Matthias F. J. Sperl:** methodology, investigation, writing – review and editing. **Christian J. Merz:** methodology, investigation, writing – review and editing. **Laura-Isabelle Klatt:** data curation, writing – review and editing. **Christoph Fraenz:** data curation, writing – review and editing. **Erhan Genç:** project administration, supervision, methodology, conceptualization, funding acquisition, data curation, writing – review and editing.

Acknowledgments

We would like to thank our student assistants, Patrick Friedrich and Helene Selpien, for supporting data recordings. We also would like to thank Tobias Otto and Dorothea Metzen for assistance with the analysis of SCR data and Marie-Christin Fellner for the establishment of simultaneous EEG/fMRI recordings.

Funding

The project was funded by a grant from the Deutsche Forschungsgemeinschaft (DFG; project number 31680338), as part of the A03 project in the "SFB 1280 Extinction Learning" Collaborative Research Centre.

Disclosure

Use of AI generated content (AIGC) and tools: We used ChatGPT (OpenAI) to improve grammar, enhance clarity, and check for cohesion at the sentence level in the manuscript. All AI-generated suggestions were reviewed and edited by the authors before inclusion in the text. The authors take full responsibility for the content of this publication.

Conflicts of Interest

The authors declare no conflicts of interest.

Data Availability Statement

The preprocessed EEG data, EDA data, contingency ratings, and the fMRI statistical maps are available at https://osf.io/w4vsh. Raw data and other materials are available upon request.

References

Abreu, R., A. Leal, and P. Figueiredo. 2018. "EEG-Informed fMRI: A Review of Data Analysis Methods." *Frontiers in Human Neuroscience* 12: 29. https://doi.org/10.3389/fnhum.2018.00029.

Åhs, F., P. A. Kragel, D. J. Zielinski, R. Brady, and K. S. LaBar. 2015. "Medial Prefrontal Pathways for the Contextual Regulation of Extinguished Fear in Humans." *NeuroImage* 122: 262–271. https://doi.org/10.1016/j.neuroimage.2015.07.051.

Allen, P. J., O. Josephs, and R. Turner. 2000. "A Method for Removing Imaging Artifact From Continuous EEG Recorded During Functional MRI." *NeuroImage* 12, no. 2: 230–239. https://doi.org/10.1006/nimg.2000.0599.

Allen, P. J., G. Polizzi, K. Krakow, D. R. Fish, and L. Lemieux. 1998. "Identification of EEG Events in the MR Scanner: The Problem of Pulse Artifact and a Method for Its Subtraction." *NeuroImage* 8, no. 3: 229–239. https://doi.org/10.1006/nimg.1998.0361.

Andres, E., B. Meyer, K. S. L. Yuen, and R. Kalisch. 2024. "Current State of the Neuroscience of Fear Extinction and Its Relevance to Anxiety Disorders." In *New Discoveries in the Brain Sciences of Fear and Anxiety – From Basic to Clinical Neuroscience*, edited by J. U. Blackford and M. R. Milad, 73–92. Springer. https://doi.org/10.1007/7854_2024_555.

Başar, E., C. Başar-Eroglu, S. Karakaş, and M. Schürmann. 2001. "Gamma, Alpha, Delta, and Theta Oscillations Govern Cognitive Processes." *International Journal of Psychophysiology* 39, no. 2–3: 241–248. https://doi.org/10.1016/S0167-8760(00)00145-8.

14698986, 2026, 3, Downloaded from https://onlinelibrary.wiley.com/doi/10.1111/psyp.70281 by Erhan Genc - Inst f Arbeitsphysiologie Dortmund , Wiley Online Library on [23/03/2026]. See the Terms and Conditions (https://onlinelibrary.wiley.com/terms-and-conditions) on Wiley Online Library for rules of use; OA articles are governed by the applicable Creative Commons License

Battaglia, S., S. Garofalo, G. di Pellegrino, and F. Starita. 2020. "Revaluing the Role of vmPFC in the Acquisition of Pavlovian Threat Conditioning in Humans." *Journal of Neuroscience* 40, no. 44: 8491–8500. https://doi.org/10.1523/JNEUROSCI.0304-20.2020.

Beckers, T., D. Hermans, I. Lange, L. Luyten, S. Scheveneels, and B. Vervliet. 2023. "Understanding Clinical Fear and Anxiety Through the Lens of Human Fear Conditioning." *Nature Reviews Psychology* 2, no. 4: 233–245. https://doi.org/10.1038/s44159-023-00156-1.

Bierwirth, P., M. I. Antov, and U. Stockhorst. 2023. "Oscillatory and Non-Oscillatory Brain Activity Reflects Fear Expression in an Immediate and Delayed Fear Extinction Task." *Psychophysiology* 60, no. 8: e14283. https://doi.org/10.1111/psyp.14283.

Bierwirth, P., M. F. J. Sperl, M. I. Antov, and U. Stockhorst. 2021. "Prefrontal Theta Oscillations Are Modulated by Estradiol Status During Fear Recall and Extinction Recall." *Biological Psychiatry: Cognitive Neuroscience and Neuroimaging* 6, no. 11: 1071–1080. https://doi.org/10.1016/j.bpsc.2021.02.011.

Blair, H. T., G. E. Schafe, E. P. Bauer, S. M. Rodrigues, and J. E. LeDoux. 2001. "Synaptic Plasticity in the Lateral Amygdala: A Cellular Hypothesis of Fear Conditioning." *Learning & Memory* 8, no. 5: 229–242. https://doi.org/10.1101/lm.30901.

Boucsein, W., D. C. Fowles, S. Grimnes, et al. 2012. "Publication Recommendations for Electrodermal Measurements." *Psychophysiology* 49, no. 8: 1017–1034. https://doi.org/10.1111/j.1469-8986.2012.01384.x.

Bouton, M. E. 2002. "Context, Ambiguity, and Unlearning: Sources of Relapse After Behavioral Extinction." *Biological Psychiatry* 52, no. 10: 976–986. https://doi.org/10.1016/S0006-3223(02)01546-9.

Bouton, M. E., S. Maren, and G. P. McNally. 2021. "Behavioral and Neurobiological Mechanisms of Pavlovian and Instrumental Extinction Learning." *Physiological Reviews* 101, no. 2: 611–681. https://doi.org/10.1152/physrev.00016.2020.

Brain Products. 2022. *Handling Scanner Related Artifacts in EEG-fMRI Studies* (Version .001) [Workshop Manual]. Brain Products Academy.

Büchel, C., and R. J. Dolan. 2000. "Classical Fear Conditioning in Functional Neuroimaging." *Current Opinion in Neurobiology* 10, no. 2: 219–223. https://doi.org/10.1016/S0959-4388(00)00078-7.

Burgos-Robles, A., I. Vidal-Gonzalez, and G. J. Quirk. 2009. "Sustained Conditioned Responses in Prelimbic Prefrontal Neurons Are Correlated With Fear Expression and Extinction Failure." *Journal of Neuroscience* 29, no. 26: 8474–8482. https://doi.org/10.1523/JNEUROSCI.0378-09.2009.

Campbell, J. I., and V. A. Thompson. 2012. "MorePower 6.0 for ANOVA With Relational Confidence Intervals and Bayesian Analysis." *Behavior Research Methods* 44, no. 4: 1255–1265. https://doi.org/10.3758/s13428-012-0186-0.

Cavanagh, J. F., and M. J. Frank. 2014. "Frontal Theta as a Mechanism for Cognitive Control." *Trends in Cognitive Sciences* 18, no. 8: 414–421. https://doi.org/10.1016/j.tics.2014.04.012.

Chen, S., Z. Tan, W. Xia, et al. 2021. "Theta Oscillations Synchronize Human Medial Prefrontal Cortex and Amygdala During Fear Learning." *Science Advances* 7, no. 34: eabf4198. https://doi.org/10.1126/sciadv.abf4198.

Chien, J. H., L. Colloca, A. Korzeniewska, et al. 2017. "Oscillatory EEG Activity Induced by Conditioning Stimuli During Fear Conditioning Reflects Salience and Valence of These Stimuli More Than Expectancy." *Neuroscience* 346: 81–93. https://doi.org/10.1016/j.neuroscience.2016.12.047.

Clarke, A., B. M. Roberts, and C. Ranganath. 2018. "Neural Oscillations During Conditional Associative Learning." *NeuroImage* 174: 485–493. https://doi.org/10.1016/j.neuroimage.2018.03.053.

Cohen, M. X. 2014. *Analyzing Neural Time Series Data: Theory and Practice*. MIT Press. https://doi.org/10.7551/mitpress/9609.001.0001.

Cohen, M. X., and T. H. Donner. 2013. "Midfrontal Conflict-Related Theta-Band Power Reflects Neural Oscillations That Predict Behavior." *Journal of Neurophysiology* 110, no. 12: 2752–2763. https://doi.org/10.1152/jn.00479.2013.

DeLaRosa, B. L., J. S. Spence, S. K. M. Shakal, et al. 2014. "Electrophysiological Spatiotemporal Dynamics During Implicit Visual Threat Processing." *Brain and Cognition* 91: 54–61. https://doi.org/10.1016/j.bandc.2014.08.003.

Dunsmoor, J. E., Y. Niv, N. Daw, and E. A. Phelps. 2015. "Rethinking Extinction." *Neuron* 88, no. 1: 47–63. https://doi.org/10.1016/j.neuron.2015.09.028.

Eklund, A., T. E. Nichols, and H. Knutsson. 2016. "Cluster Failure: Why fMRI Inferences for Spatial Extent Have Inflated False-Positive Rates." *Proceedings of the National Academy of Sciences* 113, no. 28: 7900–7905. https://doi.org/10.1073/pnas.1602413113.

Flor, H., N. Birbaumer, L. E. Roberts, et al. 1996. "Slow Potentials, Event-Related Potentials, "Gamma-Band" Activity, and Motor Responses During Aversive Conditioning in Humans." *Experimental Brain Research* 112, no. 2: 298–312. https://doi.org/10.1007/BF00227648.

Fraenz, C., D. Metzen, C. J. Merz, et al. 2025. "Fear Learning Sculpts Functional Brain Connectivity at Rest Beyond the Traditional Fear Network." *Behavioural Brain Research* 495: 115764. https://doi.org/10.1016/j.bbr.2025.115764.

Fullana, M. A., A. Albajes-Eizagirre, C. Soriano-Mas, et al. 2018. "Fear Extinction in the Human Brain: A Meta-Analysis of fMRI Studies in Healthy Participants." *Neuroscience & Biobehavioral Reviews* 88: 16–25. https://doi.org/10.1016/j.neubiorev.2018.03.002.

Fullana, M. A., B. J. Harrison, C. Soriano-Mas, et al. 2016. "Neural Signatures of Human Fear Conditioning: An Updated and Extended Meta-Analysis of fMRI Studies." *Molecular Psychiatry* 21, no. 4: 500–508. https://doi.org/10.1038/mp.2015.88.

Gershman, S. J., D. M. Blei, and Y. Niv. 2010. "Context, Learning, and Extinction." *Psychological Review* 117, no. 1: 197–209. https://doi.org/10.1037/a0017808.

Gershman, S. J., M. H. Monfils, K. A. Norman, and Y. Niv. 2017. "The Computational Nature of Memory Modification." *eLife* 6: e23763. https://doi.org/10.7554/eLife.23763.001.

Gilmartin, M. R., N. L. Balderston, and F. J. Helmstetter. 2014. "Prefrontal Cortical Regulation of Fear Learning." *Trends in Neurosciences* 37, no. 8: 455–464. https://doi.org/10.1016/j.tins.2014.05.004.

Graner, J. L., D. Stjepanović, and K. S. LaBar. 2020. "Extinction Learning Alters the Neural Representation of Conditioned Fear." *Cognitive, Affective, & Behavioral Neuroscience* 20, no. 5: 983–997. https://doi.org/10.3758/s13415-020-00814-4.

Hanslmayr, S., G. Volberg, M. Wimber, M. Raabe, M. W. Greenlee, and K. H. T. Bäuml. 2011. "The Relationship Between Brain Oscillations and BOLD Signal During Memory Formation: A Combined EEG–fMRI Study." *Journal of Neuroscience* 31, no. 44: 15674–15680. https://doi.org/10.1523/JNEUROSCI.3140-11.2011.

Hermann, C., and M. F. J. Sperl. 2023. "Classical Conditioning." In *Handbook of Clinical Child Psychology: Integrating Theory and Research Into Practice*, edited by J. L. Matson, 425–457. Springer. https://doi.org/10.1007/978-3-031-24926-6_21.

Herrmann, C. S., D. Strüber, R. F. Helfrich, and A. K. Engel. 2016. "EEG Oscillations: From Correlation to Causality." *International Journal of Psychophysiology* 103: 12–21. https://doi.org/10.1016/j.ijpsycho.2015.02.003.

Jenkinson, M., C. F. Beckmann, T. E. J. Behrens, M. W. Woolrich, and S. M. Smith. 2011. "FSL." *NeuroImage* 62, no. 2: 782–790. https://doi.org/10.1016/j.neuroimage.2011.09.015.

Kalisch, R., E. Korenfeld, K. E. Stephan, N. Weiskopf, B. Seymour, and R. J. Dolan. 2006. "Context-Dependent Human Extinction Memory Is

14698986, 2026, 3, Downloaded from https://onlinelibrary.wiley.com/doi/10.1111/psyp.70281 by Erhan Genc - Inst f Arbeitsphysiologie Dortmund , Wiley Online Library on [23/03/2026]. See the Terms and Conditions (https://onlinelibrary.wiley.com/terms-and-conditions) on Wiley Online Library for rules of use; OA articles are governed by the applicable Creative Commons License

Mediated by a Ventromedial Prefrontal and Hippocampal Network." *Journal of Neuroscience* 26, no. 37: 9503–9511. https://doi.org/10.1523/JNEUROSCI.2021-06.2006.

Karalis, N., C. Dejean, F. Chaudun, et al. 2016. "4-Hz Oscillations Synchronize Prefrontal-Amygdala Circuits During Fear Behavior." *Nature Neuroscience* 19, no. 4: 605–612. https://doi.org/10.1038/nn.4251.

Kausche, F. M., H. P. Carsten, K. M. Sobania, and A. Riesel. 2025. "Fear and Safety Learning in Anxiety-and Stress-Related Disorders: An Updated Meta-Analysis." *Neuroscience & Biobehavioral Reviews* 169: 105983. https://doi.org/10.1016/j.neubiorev.2024.105983.

Kim, J. J., and M. W. Jung. 2006. "Neural Circuits and Mechanisms Involved in Pavlovian Fear Conditioning: A Critical Review." *Neuroscience & Biobehavioral Reviews* 30, no. 2: 188–202. https://doi.org/10.1016/j.neubiorev.2005.06.005.

Klimesch, W. 2012. "Alpha-Band Oscillations, Attention, and Controlled Access to Stored Information." *Trends in Cognitive Sciences* 16, no. 12: 606–617. https://doi.org/10.1016/j.tics.2012.10.007.

Knight, D. C., C. N. Smith, D. T. Cheng, E. A. Stein, and F. J. Helmstetter. 2004. "Amygdala and Hippocampal Activity During Acquisition and Extinction of Human Fear Conditioning." *Cognitive, Affective, & Behavioral Neuroscience* 4, no. 3: 317–325. https://doi.org/10.3758/CABN.4.3.317.

Kriegeskorte, N., M. Mur, and P. A. Bandettini. 2008. "Representational Similarity Analysis—Connecting the Branches of Systems Neuroscience." *Frontiers in Systems Neuroscience* 2, no. 4: 1–28. https://doi.org/10.3389/neuro.06.004.2008.

Kuhn, M., A. M. Gerlicher, and T. B. Lonsdorf. 2022. "Navigating the Manyverse of Skin Conductance Response Quantification Approaches–A Direct Comparison of Trough-To-Peak, Baseline Correction, and Model-Based Approaches in Ledalab and PsPM." *Psychophysiology* 59, no. 9: e14058. https://doi.org/10.1111/psyp.14058.

LaBar, K. S., J. C. Gatenby, J. C. Gore, J. E. LeDoux, and E. A. Phelps. 1998. "Human Amygdala Activation During Conditioned Fear Acquisition and Extinction: A Mixed-Trial fMRI Study." *Neuron* 20, no. 5: 937–945. https://doi.org/10.1016/S0896-6273(00)80475-4.

Laing, P. A., B. Vervliet, J. E. Dunsmoor, and B. J. Harrison. 2025. "Pavlovian Safety Learning: An Integrative Theoretical Review." *Psychonomic Bulletin & Review* 32, no. 1: 176–202. https://doi.org/10.3758/s13423-024-02559-4.

Lakens, D. 2013. "Calculating and Reporting Effect Sizes to Facilitate Cumulative Science: A Practical Primer for t-tests and ANOVAs." *Frontiers in Psychology* 4: 863. https://doi.org/10.3389/fpsyg.2013.00863.

Lakens, D. 2022. "Sample Size Justification." *Collabra: Psychology* 8, no. 1: 33267. https://doi.org/10.1525/collabra.33267.

Likhtik, E., J. M. Stujenske, M. A. Topiwala, A. Z. Harris, and J. A. Gordon. 2014. "Prefrontal Entrainment of Amygdala Activity Signals Safety in Learned Fear and Innate Anxiety." *Nature Neuroscience* 17, no. 1: 106–113. https://doi.org/10.1038/nn.3582.

Lissek, S., A. S. Powers, E. B. McClure, et al. 2005. "Classical Fear Conditioning in the Anxiety Disorders: A Meta-Analysis." *Behaviour Research and Therapy* 43, no. 11: 1391–1424. https://doi.org/10.1016/j.brat.2004.10.007.

Lonsdorf, T. B., M. M. Menz, M. Andreatta, et al. 2017. "Don't Fear 'Fear Conditioning': Methodological Considerations for the Design and Analysis of Studies on Human Fear Acquisition, Extinction, and Return of Fear." *Neuroscience and Biobehavioral Reviews* 77: 247–285. https://doi.org/10.1016/j.neubiorev.2017.02.026.

Luck, S. J. 2014. *An Introduction to the Event-Related Potential Technique*. 2nd ed. MIT Press.

Lumley, T., P. Diehr, S. Emerson, and L. Chen. 2002. "The Importance of the Normality Assumption in Large Public Health Data Sets." *Annual Review of Public Health* 23, no. 1: 151–169. https://doi.org/10.1146/annurev.publhealth.23.100901.140546.

Michel, C. M., M. M. Murray, G. Lantz, S. Gonzalez, L. Spinelli, and R. Grave de Peralta. 2004. "EEG Source Imaging." *Clinical Neurophysiology* 115, no. 10: 2195–2222. https://doi.org/10.1016/j.clinph.2004.06.001.

Mikl, M., R. Mareček, P. Hluštík, et al. 2008. "Effects of Spatial Smoothing on fMRI Group Inferences." *Magnetic Resonance Imaging* 26, no. 4: 490–503. https://doi.org/10.1016/j.mri.2007.08.006.

Milad, M. R., and G. J. Quirk. 2002. "Neurons in Medial Prefrontal Cortex Signal Memory for Fear Extinction." *Nature* 420, no. 6911: 70–74. https://doi.org/10.1038/nature01138.

Milad, M. R., and G. J. Quirk. 2012. "Fear Extinction as a Model for Translational Neuroscience: Ten Years of Progress." *Annual Review of Psychology* 63, no. 1: 129–151. https://doi.org/10.1146/annurev.psych.121208.131631.

Milad, M. R., C. I. Wright, S. P. Orr, R. K. Pitman, G. J. Quirk, and S. L. Rauch. 2007. "Recall of Fear Extinction in Humans Activates the Ventromedial Prefrontal Cortex and Hippocampus in Concert." *Biological Psychiatry* 62, no. 5: 446–454. https://doi.org/10.1016/j.biopsych.2006.10.011.

Miskovic, V., and A. Keil. 2012. "Acquired Fears Reflected in Cortical Sensory Processing: A Review of Electrophysiological Studies of Human Classical Conditioning." *Psychophysiology* 49, no. 9: 1230–1241. https://doi.org/10.1111/j.1469-8986.2012.01398.x.

Mobbs, D., J. L. Marchant, D. Hassabis, et al. 2009. "From Threat to Fear: The Neural Organization of Defensive Fear Systems in Humans." *Journal of Neuroscience* 29, no. 39: 12236–12243. https://doi.org/10.1523/JNEUROSCI.2378-09.2009.

Mobbs, D., P. Petrovic, J. L. Marchant, et al. 2007. "When Fear Is Near: Threat Imminence Elicits Prefrontal-Periaqueductal Gray Shifts in Humans." *Science* 317, no. 5841: 1079–1083. https://doi.org/10.1126/science.1144298.

Mueller, E. M., C. Panitz, C. Hermann, and D. A. Pizzagalli. 2014. "Prefrontal Oscillations During Recall of Conditioned and Extinguished Fear in Humans." *Journal of Neuroscience* 34, no. 21: 7059–7066. https://doi.org/10.1523/JNEUROSCI.3427-13.2014.

Öhman, A., and U. Dimberg. 1978. "Facial Expressions as Conditioned Stimuli for Electrodermal Responses: A Case of" Preparedness"?" *Journal of Personality and Social Psychology* 36, no. 11: 1251–1258. https://doi.org/10.1037/0022-3514.36.11.1251.

Oostenveld, R., P. Fries, E. Maris, and J.-M. Schoffelen. 2011. "FieldTrip: Open Source Software for Advanced Analysis of MEG, EEG, and Invasive Electrophysiological Data." *Computational Intelligence and Neuroscience* 2011: 156869. https://doi.org/10.1155/2011/156869.

Otto, T., O. T. Wolf, and C. J. Merz. 2023. *EDA-Analysis App (5.11)*. Zenodo. https://doi.org/10.5281/zenodo.7965376.

Panitz, C., A. Keil, and E. M. Mueller. 2019. "Extinction-Resistant Attention to Long-Term Conditioned Threat Is Indexed by Selective Visuocortical Alpha Suppression in Humans." *Scientific Reports* 9, no. 1: 15809. https://doi.org/10.1038/s41598-019-52315-1.

Pearce, J. M., and G. Hall. 1980. "A Model for Pavlovian Learning: Variations in the Effectiveness of Conditioned but Not of Unconditioned Stimuli." *Psychological Review* 87, no. 6: 532–552. https://doi.org/10.1037/0033-295X.87.6.532.

Phelps, E. A., M. R. Delgado, K. I. Nearing, and J. E. LeDoux. 2004. "Extinction Learning in Humans." *Neuron* 43, no. 6: 897–905. https://doi.org/10.1016/j.neuron.2004.08.042.

Pitkanen, A. 2000. "Connectivity of the Rat Amygdaloid Complex." In *The Amygdala: A Functional Analysis*, edited by J. P. Aggleton, 31–115. Oxford University Press. https://doi.org/10.1093/oso/9780198505013.003.0002.

14698986, 2026, 3, Downloaded from https://onlinelibrary.wiley.com/doi/10.1111/psyp.70281 by Erhan Genc - Inst f Arbeitsphysiologie Dortmund , Wiley Online Library on [23/03/2026]. See the Terms and Conditions (https://onlinelibrary.wiley.com/terms-and-conditions) on Wiley Online Library for rules of use; OA articles are governed by the applicable Creative Commons License

Quirk, G. J., and D. Mueller. 2008. "Neural Mechanisms of Extinction Learning and Retrieval." *Neuropsychopharmacology* 33, no. 1: 56–72. https://doi.org/10.1038/sj.npp.1301555.

Radua, J., H. S. Savage, E. Vilajosana, et al. 2025. "Neural Correlates of Human Fear Conditioning and Sources of Variability in 2199 Individuals." *Nature Communications* 16, no. 1: 7869. https://doi.org/10.1038/s41467-025-63078-x.

Rescorla, R. A. 1967. "Pavlovian Conditioning and Its Proper Control Procedures." *Psychological Review* 74, no. 1: 71–80. https://doi.org/10.1037/h0024109.

Rescorla, R. A. 1988. "Pavlovian Conditioning: It's Not What You Think It Is." *American Psychologist* 43, no. 3: 151–160. https://doi.org/10.1037/0003-066X.43.3.151.

Rescorla, R. A., and A. R. Wagner. 1972. "A Theory of Pavlovian Conditioning: Variations in the Effectiveness of Reinforcement and Non Reinforcement." In *Classical Conditioning II: Current Research and Theory*, edited by A. H. Black and W. F. Prosaky, 64–99. Appleton-Century- Crofts.

Ressler, K. J. 2020. "Translating Across Circuits and Genetics Toward Progress in Fear-and Anxiety-Related Disorders." *American Journal of Psychiatry* 177, no. 3: 214–222. https://doi.org/10.1176/appi.ajp.2020.20010055.

Rorden, C. 2025. "MRIcroGL: Voxel-Based Visualization for Neuroimaging." *Nature Methods* 22, no. 8: 1613–1614. https://doi.org/10.1038/s41592-025-02763-7.

Sehlmeyer, C., S. Schöning, P. Zwitserlood, et al. 2009. "Human Fear Conditioning and Extinction in Neuroimaging: A Systematic Review." *PLoS One* 4, no. 6: e5865. https://doi.org/10.1371/journal.pone.0005865.

Seidenbecher, T., T. R. Laxmi, O. Stork, and H.-C. Pape. 2003. "Amygdalar and Hippocampal Theta Rhythm Synchronization During Fear Memory Retrieval." *Science* 301, no. 5634: 846–850. https://doi.org/10.1126/science.1085818.

Sjouwerman, R., J. Niehaus, and T. B. Lonsdorf. 2015. "Contextual Change After Fear Acquisition Affects Conditioned Responding and the Time Course of Extinction Learning—Implications for Renewal Research." *Frontiers in Behavioral Neuroscience* 9: 337. https://doi.org/10.3389/fnbeh.2015.00337.

Smith, S. M., M. Jenkinson, M. W. Woolrich, et al. 2004. "Advances in Functional and Structural MR Image Analysis and Implementation as FSL." *NeuroImage* 23: S208–S219. https://doi.org/10.1016/j.neuroimage.2004.07.051.

Somers, J. M., E. M. Goldner, P. Waraich, and L. Hsu. 2006. "Prevalence and Incidence Studies of Anxiety Disorders: A Systematic Review of the Literature." *Canadian Journal of Psychiatry* 51, no. 2: 100–113. https://doi.org/10.1177/070674370605100206.

Sperl, M. F. J., C. Panitz, C. Hermann, and E. M. Mueller. 2016. "A Pragmatic Comparison of Noise Burst and Electric Shock Unconditioned Stimuli for Fear Conditioning Research With Many Trials." *Psychophysiology* 53, no. 9: 1352–1365. https://doi.org/10.1111/psyp.12677.

Sperl, M. F. J., C. Panitz, I. M. Rosso, et al. 2019. "Fear Extinction Recall Modulates Human Frontomedial Theta and Amygdala Activity." *Cerebral Cortex* 29: 701–715. https://doi.org/10.1093/cercor/bhx353.

Sperl, M. F. J., A. Wroblewski, M. Mueller, B. Straube, and E. M. Mueller. 2021. "Learning Dynamics of Electrophysiological Brain Signals During Human Fear Conditioning." *NeuroImage* 226: 117569. https://doi.org/10.1016/j.neuroimage.2020.117569.

Starita, F., G. Pirazzini, G. Ricci, et al. 2023. "Theta and Alpha Power Track the Acquisition and Reversal of Threat Predictions and Correlate With Skin Conductance Response." *Psychophysiology* 60, no. 7: e14247. https://doi.org/10.1111/psyp.14247.

Steiger, J. H. 2004. "Beyond the F Test: Effect Size Confidence Intervals and Tests of Close Fit in the Analysis of Variance and Contrast Analysis." *Psychological Methods* 9, no. 2: 164–182. https://doi.org/10.1037/1082-989x.9.2.164.

Totty, M. S., T. Tuna, K. R. Ramanathan, J. Jin, S. E. Peters, and S. Maren. 2023. "Thalamic Nucleus Reuniens Coordinates Prefrontal-Hippocampal Synchrony to Suppress Extinguished Fear." *Nature Communications* 14, no. 1: 6565. https://doi.org/10.1038/s41467-023-42315-1.

VanElzakker, M. B., M. Kathryn Dahlgren, F. Caroline Davis, S. Dubois, and L. M. Shin. 2014. "From Pavlov to PTSD: The Extinction of Conditioned Fear in Rodents, Humans, and Anxiety Disorders." *Neurobiology of Learning and Memory* 113: 3–18. https://doi.org/10.1016/j.nlm.2013.11.014.

Visser, R. M., J. Bathelt, H. S. Scholte, and M. Kindt. 2021. "Robust BOLD Responses to Faces but Not to Conditioned Threat: Challenging the Amygdala's Reputation in Human Fear and Extinction Learning." *Journal of Neuroscience* 41, no. 50: 10278–10292. https://doi.org/10.1523/JNEUROSCI.0857-21.2021.

Wake, S., N. Hedger, C. M. Van Reekum, and H. Dodd. 2024. "The Effect of Social Anxiety on Threat Acquisition and Extinction: A Systematic Review and Meta-Analysis." *PeerJ* 12: e17262. https://doi.org/10.7717/peerj.17262.

Wen, Z., Z. S. Chen, and M. R. Milad. 2021. "Fear Extinction Learning Modulates Large-Scale Brain Connectivity." *NeuroImage* 238: 118261. https://doi.org/10.1016/j.neuroimage.2021.118261.

Wen, Z., E. F. Pace-Schott, S. W. Lazar, et al. 2024. "Distributed Neural Representations of Conditioned Threat in the Human Brain." *Nature Communications* 15, no. 1: 2231. https://doi.org/10.1038/s41467-024-46508-0.

Wen, Z., C. M. Raio, E. F. Pace-Schott, et al. 2022. "Temporally and Anatomically Specific Contributions of the Human Amygdala to Threat and Safety Learning." *Proceedings of the National Academy of Sciences* 119, no. 26: e2204066119. https://doi.org/10.1073/pnas.2204066119.

Yin, S., K. Bo, Y. Liu, N. Thigpen, A. Keil, and M. Ding. 2020. "Fear Conditioning Prompts Sparser Representations of Conditioned Threat in Primary Visual Cortex." *Social Cognitive and Affective Neuroscience* 15, no. 9: 950–964. https://doi.org/10.1093/scan/nsaa122.

Zhang, Y., J. Lin, H. Dou, H. Zhang, Y. Cao, and Y. Lei. 2025. "Modulation of Fear Extinction by Non-Invasive Brain Stimulation: Systematic Review and Meta-Analysis." *Psychophysiology* 62, no. 2: e14763. https://doi.org/10.1111/psyp.14763.

Zinbarg, R. E., A. L. Williams, and S. Mineka. 2022. "A Current Learning Theory Approach to the Etiology and Course of Anxiety and Related Disorders." *Annual Review of Clinical Psychology* 18, no. 1: 233–258. https://doi.org/10.1146/annurev-clinpsy-072220-021010.

Supporting Information

Additional supporting information can be found online in the Supporting Information section. **Figure S1:** dB-normalized EEG theta dynamics from frontomedial electrodes (F1, Fz, and F2) during fear acquisition and extinction training across three trial segments (0 to 2 s, 2 to 4 s, and 4 to 5.5 s post-CS), during *first half* (trials 1–8 in acquisition training; trials 1–4 in extinction training) and *second half* (trials 9–16 in acquisition training; trials 5–8 in extinction training). The error bars represent 95% CIs around the means. The significant CS+ > CS− differences in specific trial segments are marked with asterisks (**$p < 0.01$, *$p < 0.05$). **Figure S2:** Results of the fMRI analysis without EEG parameters for the CS+ > CS− contrast during fear acquisition training, plotted on the transparent MNI152 template. The color bar codes the thresholded z statistic values from 3.1 to 4.1 in the significant cluster for the CS+ > CS− contrast, centred in the dorsal-anterior cingulate cortex (dACC) — a classical brain area of the so-called "fear network", which has also been reported in a majority of other studies (for a meta-analysis, see Fullana et al. 2016). The CS− > CS+ contrast was not significant. **Figure S3:** Reaction to the US delivery (i.e., the unconditioned

14698986, 2026, 3, Downloaded from https://onlinelibrary.wiley.com/doi/10.1111/psyp.70281 by Ethan Genc - Inst f Arbeitsphysiologie Dortmund , Wiley Online Library on [23/03/2026]. See the Terms and Conditions (https://onlinelibrary.wiley.com/terms-and-conditions) on Wiley Online Library for rules of use; OA articles are governed by the applicable Creative Commons License

response), contrasted with a similar time point during the CS− trials. Voxelwise statistical maps are overlaid on the MNI152 2 mm template. The color bar codes the thresholded *z*-statistic values from 3.1 to 6.1 (this is in contrast to other brain maps in the main manuscript, where the color bar ranges from 3.1 to 4.1). Whole-brain analysis revealed a robust activation in bilateral insula, dorsal-anterior cingulate cortex (dACC), left precentral gyrus, bilateral angular gyri, left primary somatosensory cortex, bilateral opercula, and the whole cerebellum. *Activation in the left primary somatosensory cortex during the US delivery period (middle axial slice) shows, as anticipated, a contralateral response to the US, which was delivered to the right hand*. **Figure S4:** The trial-by-trial skin conductance responses (SCRs) averaged for all participants during fear acquisition training ($N = 35$) and extinction training ($N = 32$). The error bars denote the 95% confidence interval around the mean across participants. The significant CS+ > CS− differences in specific trials are marked with asterisks (**$p < 0.01$, *$p < 0.05$).

14698986, 2026, 3, Downloaded from https://onlinelibrary.wiley.com/doi/10.1111/psyp.70281 by Erhan Genc - Inst f Arbeitsphysiologie Dortmund , Wiley Online Library on [23/03/2026]. See the Terms and Conditions (https://onlinelibrary.wiley.com/terms-and-conditions) on Wiley Online Library for rules of use; OA articles are governed by the applicable Creative Commons License